ผลของสภาวะในการเผาต่อสมบัติความชอบน้ำของฟิล์มไททาเนียมไดออกไซด์

นายศุภวุฒิ ภู่ภัทรกุล

EFFECT OF CALCINATION CONDITIONS ON HYDROPHILICITY OF TITANIUM DIOXIDE FILMS

Mr. Supawut Phuphattarakul

Thesis Title	EFFECT OF CALCINATION CONDITIONS ON HYDROPHILICITY OF TITANIUM DIOXIDE FILMS
By	Mr. Supawut Phuphattarakul
Field of Study	Chemical Engineering
Thesis Advisor	Akawat Sirisuk, Ph.D.
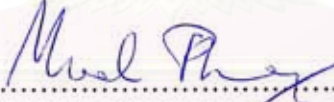
Accepted by the Faculty of Engineering, Chulalongkorn University in Partial Fulfillment of the Requirements for the Master's Degree

....Dean of the Faculty of Engineering

(Professor Direk Lavansiri, Ph.D.)

THESIS COMMITTEE

....Chairman

(Professor Piyasarn Praserthdam, Dr. Ing)

.... Thesis Advisor

(Akawat Sirisuk, Ph.D.)

.... Member

(Assistant Professor Muenduen Phisalaphong, Ph.D.)

..................................Member

(Assistant Professor Joongjai Panpranot, Ph.D.)

ศุวภวุฒิ ภู่ภัทรกุล: ผลของสภาวะในการเผาต่อสมบัติความชอบน้ำของฟิล์มไทเทเนียมได
ออกไซด์ (EFFECT OF CALCINATION CONDITIONS ON
HYDROPHILICITY OF TITANIUM DIOXIDE FILMS) อ. ที่ปรึกษา: ดร.อัคร
วัต ศิริสุข, 53 หน้า, ISBN: 974–17-4324-6

ไทเทเนียมไดออกไซด์สามารถเตรียมได้โดยวิธีโซล-เจล โดยใช้ ไทเทเนียมไอโซโพรพรอก
ไซด์เป็นสารตั้งต้น กระจกโบโรซิลิเกตถูกนำมาใช้เป็นแผ่นรองรับไทเทียมไดออกไซด์ ตัวอย่างจะถูก
นำมาเผาในสภาวะที่แตกต่าง ซึ่งได้แก่ อุณหภูมิและบรรยากาศที่ใช้ในการเผาเพื่อศึกษาสมบัติ
ความชอบน้ำของแผ่นฟิล์มไทเทเนีย ผลการศึกษาพบว่าฟิล์มไทเทเนียที่เผาที่อุณหภูมิ 550 องศา
เซลเซียสในการเผาในที่อากาศนิ่งให้ค่ามุมสัมผัสที่คงตัวต่ำที่สุด เมื่ออุณหภูมิในการเผาลดลงทำ
ให้ค่ามุมสัมผัสที่คงตัวสูงขึ้น อุณหภูมิในการเผาที่เพิ่มขึ้นจะทำให้ปริมาณของไทเทเนียมไอออน
สามบวกและรูไทล์เฟส ผลของบรรยากาศในการเผา การเผาในที่อากาศนิ่งให้ค่ามุมสัมผัสที่คงตัว
ต่ำที่สุดอาจเป็นผลมาจากปริมาณของไทเทเนียมไอออนสามบวกบนพื้นผิวที่สูง

การปรับปรุงสภาพพื้นผิวของตัวอย่างทำได้โดยกระบวนการเผาในสองขั้นตอน ขั้นแรก
เป็นการเผาภายใต้อากาศเพื่อเปลี่ยนไทเทเนียที่อยู่ในรูปอสัณฐานเป็นผลึก จากนั้นการเผาซ้ำใน
บรรยากาศของไฮโดรเจนเพื่อเพิ่มไทเทเนียมไอออนสามบวก พบว่าการเผาในสองขั้นตอนจะให้ค่า
มุมสัมผัสที่ลดลงแม้ว่าจะว่าจะเผาที่อุณหภูมิต่ำลงเมื่อเปรียบเทียบกับการเผาเพียงขั้นตอนเดียว

ภาควิชา..... ....วิศวกรรมเคมี.............	ลายมือชื่อนิสิต..................	
สาขาวิชา.......วิศวกรรมเคมี..............	ลายมือชื่ออาจารย์ที่ปรึกษา...................	

ปีการศึกษา..... .2548.....................

##4770479221: MAJOR CHEMICAL ENGINEERING

KEY WORD: TITANIA / TITANIUM (IV) OXIDE THIN FILMS / SOL-GEL METHOD / SUPERHYDROPHILIC / CALCINATION / DEFECT

SUPAWUT PHUPHATTARAKUL: EFFECT OF CALCINATION CONDITIONS ON HYDROPHILICITY OF TITANIUM DIOXIDE FILMS THESIS ADVISOR: AKAWAT SIRISUK, Ph.D. 53 pp. ISBN 974-17-4324-6

Titanium dioxide was prepared via a sol-gel method using titanium isopropoxide as a precursor. Borosilicate glass slide was employed as a support for titanium dioxide thin film. Calcination conditions, namely, calcination temperature and calcination atmosphere, were varied to investigate their effects on hydrophilic property of TiO_2 thin films. Titania thin film that was calcined under stagnant air at 550 $^{\circ}$C possessed the smallest saturated contact angle. As calcination temperature decreased, the saturated contact angle of the sample grew larger. The increase was attributed to lower Ti^{3+} surface defect and the presence of less rutile phase in the sample. Regarding calcination atmosphere, the smallest saturated contact angle was observed in the sample that was calcined under stagnant air probably due to the highest Ti^{3+} surface defect.

Then further surface modification of the sample was done by employing two-step calcination process. The first step involved calcination under air flow so as to transform amorphous titania to titania crystals. Then, the sample was calcined under hydrogen flow in the second step to create more Ti^{3+} surface defect. We found that smaller saturated contact angle could be obtained even at a lower calcination temperature by using the two-step calcination process, when compared to the single-step calcination process.

Department........Chemical Engineering….. Student's signature……………………

Field of study….Chemical Engineering….. Advisor's signature……………………

Academic year…2005……………………....

ACKNOWLEDGEMENTS

CONTENTS

Page

LIST OF TABLES

LIST OF FIGURES

CHAPTER I

INTRODUCTION

Titanium dioxide (TiO_2) or titania, is widely used in many applications such as photcatalysis, self-cleaning surface, UV absorption, pigment, gas sensor or coating. The TiO_2 coating exhibits hydrophilic property when it is irradiated with UV light. This property is called "photo-induced hydrophilicity". This effect was discovered accidentally in work by TOTO Inc. in 1995. Since then, many researchers (Wang *et al.*,1997; Fujishima *et al.*,2001; Yu *et al.*,2001) tried to explain its mechanism. This process is similar to a photocatalytic process that holes and electrons can be separated when it is excited by energy of UV light and migrate to the titanium dioxide surface. However, this process is different in the role of hole that causes oxygen vacancy and hydrophilic surface.

The synthesis of nanosized titania includes a number of techniques such as precipitation, chemical vapor deposition, solvothermal method, and glycothermal method. One of the techniques used for synthesis of titania is a sol-gel method. This method can produce nanosized titania at room temperature without consuming a great deal of energy. Furthermore, titania sol can be coated on a substrate directly by wet process such as dip coating, spin coating or spray coating. These coating techniques use simple principle so they are widely utilized for film experiment.

There are many factors that affect to photo-induced hydrophilicity of titanium dioxide, including phase structure, Ti^{3+} and OH group. It is well known that the different phase structure gives rise to the different properties of titanium dioxide such as photocatalytic activity. However, there are no evidences to prove that this factor affects photo-induced hydrophilicity directly. While in the cases of Ti^{3+} and OH group, that the more the amount of Ti^{3+} and OH group, the more the photo-induced hydrophilic property. Therefore, it may be the other factors such as crystalline site of TiO_2, specific surface area or morphology.

In this research we focus on the study of effects of calcination conditions on properties and photo-induced hydrophilicity of titanium dioxide film which is prepared by using a sol-gel method.

The objectives of this research are as follows:

1. To study the effects of calcination conditions on photo-induced hydrophilicity of TiO_2, which is prepared via a sol-gel method.

2. To study the effect of surface modification by treating with various gases during heat treatment on photo-induced hydrophilicity of TiO_2.

This thesis is arranged as follows:

Chapter II presents literature reviews of previous works related to this research.

Chapter III explains basic information about titania and also discusses principles of photo-induced hydrophilicity.

Chapter IV describes synthesis of titania and preparation of titania thin film employed in this research and experimental apparatus and setting.

Chapter V presents experimental results and discussion.

Chapter VI presents overall conclusions of this research and recommendations for future research.

CHATPTER II

LITERATURE REVIEWS

2.1 Titanium dioxide for use as hydrophilic material

2.1.1 Effect of titanium dioxide phase structure

G. Yanfeng and coworkers (2004) studied photo-induced superhydrophilicity of amorphous titanium dioxide prepared by the peroxotitanate-complex deposition (PCD) and liquid-phase deposition (LPD) methods at room temperature. The contact angles of PCD and LPD thin films before UV irradiated were 66° and 34° respectively. After five-minute irradiation, both films showed superhydrophilicity, where the contact angle become zero. This result could explain that concentration of broken bonds and other defects related to Ti^{3+} were larger than crystalline form.

T. Watanabe and coworkers (1999) studied the different plane of rutile single crystal and polycrystalline anatase titanium dioxide. Anatase polycrystalline was prepared by sol-gel method on soda lime glass that was coated with a silicon dioxide layer and was fired in air at 500 ^{o}C for 20 minutes. The (110) surface of rutile single crystal had bridging site oxygens, which was more reactive, but not on the (001) surface so the rate of decreasing contact angle, saturated contact angle and conversion rate of hydrophilicity to hydrophobicity of (110) were better.

J.M. Yu and coworkers (2002) studied two different structures of titanium dioxide. They used reverse micellar and sol-gel methods to synthesize mesoporous TiO_2 ($MTiO_2$) and TiO_2 thin films respectively. TiO_2 thin films were calcined at 500 and 900 ^{o}C to obtain two different phase structures, anatase and rutile respectively. The result for both $MTiO_2$ and TiO_2 indicated that anatase phase was more hydrophilic than rutile phase.

2.2.2 Effect of Ti^{3+}

Lee and coworkers (2003) investigated effect of doping of aluminium (Al), tungsten (W) and both aluminium and tungsten (Al+W). TiO$_2$ thin film was coated on soda lime glass and quartz substrates using a dip technique. Then the films were baked at 150 ^{o}C and annealed at 500 ^{o}C. Doping of either Al or W brought about a slight decrease in contact angle (40° and 25°) after being irradiated for long time, while doping two metal gave rise to the lowest contact angle (5°). The some trend was observed for both types of substrate. XPS ananlysis revealed that concentration of Ti^{3+} on TiO$_2$ surface was a major factor influencing hydrophilicity. The concentrations of Ti^{3+} in undoped, Al-doped, W-doped and Al+W-doped were 58.63%, 46.45%, 57.91 % and 63.81% (Ti^{3+}/Ti^{4+}), respectively. Furthermore, hydrophilicity of titanium dioxide depended on traps for electrons or holes and surface acidity.

2.2.3 Effect of OH group

Y. Jiaguo and Z. Xiujian (2001) studied the effect of surface microstructure on superhydrophilic property of TiO$_2$ thin film prepared by a sol-gel method. Polyethylene glycol (PEG) was added to improve properties of film. When amount of PEG increased, pore sizes of the film became larger. The addition of PEG increased surface hydroxyl groups, which resulted in greater hydrophilicity. However, when amount of PEG reached 0.5 g, the contact angle of titania thin film remain unchanged.

Y. Jiaguo and Z. Xiujian (2002) studied the difference between TiO$_2$ thin films before and after treatment with hydrochloric acid (HCl). Titanium dioxide was coated on glass substrate and was heated at 500 ^{o}C for one hour. Then the sample was soaked in 0.2 M HCl for four days. This result showed that thickness of TiO$_2$ film did not affect superhydrophilicity. Moreover, XPS analysis indicated that hydroxyl group of treated TiO$_2$ film increased and led to a decrease in contact angle.

2.2 Effect of surface modification to TiO_2 structure.

H. Liu and coworkers (2002) investigated structure of titanium dioxide powder calcined under hydrogen atmosphere at a high temperature as a pretreatment. The in situ electron paramagnetic resonance (EPR) signals revealed the increased intensity of Ti^{3+} peak at ca. 600 ^{o}C. Meanwhile, intensity of oxygen vacancy (OV) increased in the range of 450 – 520 ^{o}C too. However, only the effect of increased Ti^{3+} on was reported, not the photo-induced hydrophilicity of TiO_2 film.

K. Suriye and coworkers (2005) studied the effect of calcinations atmosphere for TiO_2. Titania was prepared by a sol-gel method was then calcined under nitrogen and oxygen atmosphere at various compostion to alter the surface defect (Ti^{3+}) concentration. Both the CO_2-temperature programmed desoprtion and electron spin resonance indicated that the amount of surface defects increased with the increasing amount of oxygen in the calcination atmosphere. Calcination under pure hydrogen atmosphere brought about the highest amount of defects.

F. Guillemot and coworkers (2002) studied the effect of temperature on defect surface defects. Titania samples were purchased from a commercial source. Titanium dioxide sample was analyzed by X-ray photoelectron spectroscopy after in situ heating in the range of 323 – 573 K for eight hours. The surface defect density (Ti^{3+}/Ti^{4+}) of a sample was less than 3% at 323 K and increased to 21% at 573 K. Furthermore, annealing at a temperature above 600 K still fewer surface defects caused Ti^{3+} damaged to the structure.

J.E. Rekoske and M.A. Barteau (1997) investigated the effect of calcination under hydrogen atmosphere on the mass change upon reduction rate of titania. Titania samples were obtained from commercial sources in the experiment. The mass loss corresponded to oxygen loss from titania structure or oxygen vacancies. Calcination temperature was varied in the range of 573 to 773 K. At 573 K oxygen loss rate decreased slightly while at higher calcination temperature, these rates droped dramatically during 30 minutes then decreased gradually. The oxygen vacancies or Ti^{3+} defects for both anatase and rutile were proportional to the calcination temperature.

G. Lu and coworkers (1994) studied the creation of surface oxygen vacancies (defects) on TiO_2 (110) surface by thermal annealing at high temperature (500 to 900 K). Titania sample was obtained from commercial source. Ti^{3+} defect sites were detected by temperature programmed desorption using CO_2. The higher annealing temperature, the more Ti^{3+} defect sites. Furthermore, these Ti^{3+} sites was a result of the loss of bridging oxygen atom on the TiO_2 (110) surface.

CHAPTER III

THEORY

This chapter consists of three main sections. Section 3.1 discusses properties and applications of materials used in the research. Synthesis of such materials by sol-gel method is described in Section 3.2. Details on photo-induced hydrophilicity processes are discussed in Section 3.3. Definition of contact angle and classification of hydrophilic and hydrophobic described in Section 3.4.

3.1 Titanium dioxide

This section discusses properties and applications of titanium dioxide. This material was employed to coat glass substrates to be tested for photo-induced hydrophilicity.

3.1.1 Physical and Chemical Properties (Othmer, 1991; Fujishima *et al.*, 1999)

Titanium dioxide may take on any of the following three crystal structures: anatase, which tends to be more stable at low temperature; brookite, which is usually found only in minerals; and rutile, which tends to be more stable at higher temperatures and thus is sometimes found in igneous rock.

Anatase generally shows a higher photocatalytic activity than the other types of titanium dioxide. Comparison of same physical properties of rutile and anatase is shown in Table 3.1.

Table 3.1 Comparison of rutile, brookite and anatase. (Othmer, 1991 and Fujishima *et al.*, 1999).

Properties	Anatase	Brookite	Rutile
Crystal structure	Tetragonal	Orthorhombic	Tetragonal
Optical	Uniaxial, negative	Biaxial, positive	Uniaxial, negative
Density, g/cm^3	3.9	4.0	4.23
Harness, Mohs scale	$5^1/_2 - 6$	$5^1/_2 - 6$	$7 - 7^1/_2$
Unit cell	$D_4a^{19}.4TiO_2$	$D_2h^{15}.8TiO_2$	$D_4h^{12}.3TiO_2$
Dimension, nm			
a	0.3758	0.9166	0.4584
b	-	0.5436	-
c	0.9514	0.5135	2.953
Refractive index	2.52	-	2.52
Permittivity	31	-	114
Melting point	changes to rutile at high temperature	-	1858˚C

The reason that anatase is more photoactive than rutile may lie in the differences in their so-called energy band structures. The band gap energy of a semiconductor is the minimum energy of light required to make the material electrically conductive or, in other words, to get the electrons excited enough to get moving. The band gap energy of anatase is 3.2 eV, which corresponds to UV light with wavelength of 388 nanometers, while the band gap energy for the rutile type is 3.0 eV, corresponding to violet light that has a wavelength of 413 nanometers. The level of the conduction band for anatase is 0.2 eV higher than that for rutile. In more technical terminology, the band gap energy for a semiconductor indicates the

minimum energy of light necessary to produce electrons in the conduction band (CB) and give rise to electrical conductivity (photoconductivity) and "holes," which are actually the absence of electrons, in the valence band (VB). These holes can react with water to produce the highly reactive hydroxyl radical ($\bullet$OH). Both holes and hydroxyl radicals can oxidize most organic materials.

The VB energies for both anatase and rutile are very low in the energy. Consequently, the VB holes (and the hydroxyl radicals) have great oxidizing power. The CB energy for rutile is close to the potential required to electrolytically reduce water to hydrogen gas, but that for anatase is higher in the energy, meaning that it has higher reducing power. Therefore, anatase can drive the very important reaction involving the electrolytic reduction of molecular oxygen (O_2) to superoxide ($O_2\bullet^-$).

Although anatase and rutile are both tetragonal, they don't have the same crystal structures. Anatase exists in near-regular octahedral and rutile forms slender prismatic crystal. Rutile is the thermally stable form and is one of the two most important ores of titanium.

The three forms of titanium (IV) oxide have been prepared in laboratories but only rutile, the thermally stable form, has been obtained in the form of transparent large single crystal. The transformation from anatase to rutile is accompanied by the evolution of ca. 12.6 kJ/mol (3.01 kcal/mol), but the rate of transformation is greatly affected by temperature and by the presence of other substance which may either catalyze or inhibit the reaction. The lowest temperature at which conversion of anatase to rutile takes place at a measurable rate is around 700°C, but this is not a transition temperature. The change is not reversible since ΔG for the change from anatase to rutile is always negative.

Brookite has been produced by heating amorphous titanium (IV) oxide, which is prepared from an alkyl titanate or sodium titanate, with sodium or potassium hydroxide in an autoclave at 200 to 600°C for several days. The important commercial forms of titanium (IV) oxide are anatase and rutile, and they can readily be distinguished by X-ray diffraction spectrometry.

Since both anatase and rutile are tetragonal, they are both anisotropic, and their physical properties, e.g. refractive index, vary according to the direction relative to the crystal axes. In most applications of these substances, the distinction between crystallographic direction is lost because of the random orientation of large numbers of small particles, and only average values of the properties are significant.

(a)   (b)
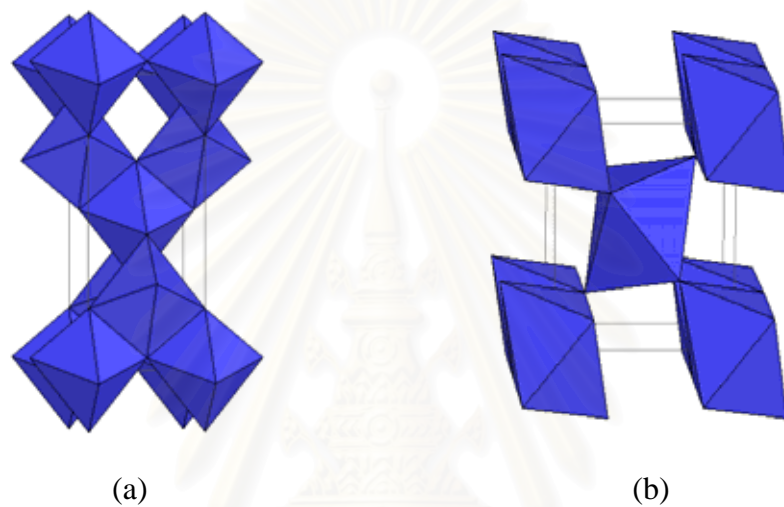
Fig 3.1 Structure of TiO_2 anatase (a) and rutile (b) phase

Measurement of physical properties, in which the crystallographic directions are taken into account, may be made for both natural and synthetic rutile, natural anatase crystals, and natural brookite crystals. Measurements of the refractive index of titanium (IV) oxide must be made by using a crystal that is suitably orientated with respect to the crystallographic axis as a prism in a spectrometer. Crystals of suitable size of all three modifications occur naturally and have been studied. However, rutile is the only form that can be obtained in large artificial crystals from melts. The refractive index of rutile is 2.75. The dielectric constant of rutile varies with direction in the crystal and with any variation from the stoichiometric formula, TiO_2; an average value for rutile in powder from is 114. The dielectric constant of anatase powder is 48.

Titanium (IV) oxide is thermally stable (mp 1855 °C) and very resistant to chemical attack. When it is heated strongly under vacuum, there is a slight loss of oxygen corresponding to a change in composition to $TiO_{1.97}$. The product is dark blue but reverts to the original white color when it is heated in air.

Hydrogen and carbon monoxide reduce it only partially at high temperatures, yielding lower oxides or mixtures of carbide and lower oxides. At ca. 2000 °C and under vacuum, carbon reduces it to titanium carbide. Reduction by metal, e.g., Na, K, Ca, and Mg, is not complete. Chlorination is only possible if a reducing agent is present; the position of equilibrium in the system is

$$TiO_2 \;+\; 2Cl_2 \qquad \rightarrow \qquad TiCl_4 \;+\; O_2$$

3.1.2 Applications of titanium dioxide

Titanium dioxide is one of the most basic materials in our daily life. Titanium dioxide has been widely used in a variety of paints, plastics, paper, inks, fibers, cosmetics, sunscreens and foodstuffs.

Naturally, the type of titanium dioxide that is used as a pigment is different from that used as a photocatalyst. The photocatalytic technology is becoming more and more attractive to industries today because environmental pollution has been recognized as a serious problem that needs to be addressed immediately. Various applications in which research and development activities involving titanium dioxide have been investigated, such as fog-proof, anti-bacterial, anti-viral, fungicidal, anti-soiling, self-cleaning, deodorizing, air purification, anti-cancer, water treatment and water purification.

3.2 Sol-gel method (Fu *et al.*, 1996; Su *et al.*, 2004)

This process occurs in liquid solution of organometallic precursors such as tetraethyl orthosilicate, zirconium propoxide and titanium isopropoxide, which, by means of hydrolysis and condensation reaction, lead to the formation of sol.

$$M\text{-}O\text{-}R \ + \ H_2O \qquad \Rightarrow \qquad M\text{-}OH \ \ + \ R\text{-}OH \qquad \text{(hydrolysis)} \qquad (3.1)$$

$$M\text{-}O\text{-}H \ + \ HO\text{-}M \qquad \Rightarrow \qquad M\text{-}O\text{-}M \ \ + \ H_2O \qquad \text{(water condensation)} \ (3.2)$$

$$M\text{-}O\text{-}R \ + \ HO\text{-}M \qquad \Rightarrow \qquad M\text{-}O\text{-}M \ \ + \ R\text{-}OH \qquad \text{(alcohol condensation)} \ (3.3)$$

A typical example of a sol-gel method is the addition of metal alkoxides to water. The alkoxides are hydrolyzed giving the oxide as a colloidal product.

The sol is made of solid particles of a diameter of few hundred nanometers suspending in a liquid phase. After that, the particles condense into gel, in which solid macromolecules are immersed in a liquid phase. Drying the gel at low temperature (25-100°C) produces porous solid matrices or xerogels. To obtain a final product, the gel is heated. This heat treatment serves several purposes, *i.e.*, to remove solvent, to decompose anions such as alkoxides or carbonates to give oxides, to rearrange of the structure of the solid, and to allow crystallization to occur.

Using the sol-gel method, one can easily control a stoichiometry of solid solution and a homogeneous distribution of nanoparticles and metal oxides. In addition, the advantages are that the metal oxides are prepared easily at room temperature and high purity can be obtained.

3.3 Theory of photo-induced hydrophilicity (Fujishima *et at.,* 2000)

The primary process involving photo-induced hydrophilicity occurs upon irradiation of a semiconductor. A semiconductor is characterized by an electronic band structure, in which the highest occupied energy band, or valence band, and the lower empty band, conduction band, are separated by a band gap. The magnitude of the energy of band gap between the electronically populated valence

band and the largely vacant conduction band governs the extent of thermal population of the conduction band in its intrinsic state. The band gap defines the wavelength sensitivity of the semiconductor to irradiation (Fox and Dulay, 1993). A photon of energy higher than or equal to the band gap energy is absorbed by a semiconductor particle. Then an electron from the valence band is promoted to the conduction band with simultaneous generation of an electronic vacancy or "hole" (h^+) in the valence band. This process is photoexcitation of electrons. Figure 3.2 shows the photocatalytic process occurring on an irradiated semiconductor particle.

In most materials that are electrically conductive, i.e., metals, two types of charge carriers, electrons (e^-) and holes (h^+), immediately recombine on the surface or the bulk of particle in a few nanoseconds and the accompanying energy is dissipated as heat (see Equation 3.4). On semiconductor such as titanium dioxide, however, the change carriers survive for longer periods of time to allow themselves to be trapped in surface states where they can react with donor (D) or acceptor (A) species adsorbed or close to the surface of the particle (Equations 3.5, 3.6, and 3.7) (Litter, 1999). Subsequently, oxidation and reduction can be initiated.

$$\text{Recombination} \qquad h^+ \;+\; e^- \;\rightarrow\; heat \qquad\qquad (3.4)$$

$$\text{Photoexcitation} \qquad Semiconductor \;+\; h\nu \;\rightarrow\; e^- + h^+ \qquad (3.5)$$

$$4h^+ \;+\; O_2^{2-} \;\rightarrow\; O_2 \qquad\qquad (3.6)$$

$$e^- \;+\; Ti^{4+} \;\rightarrow\; Ti^{3+} \qquad\qquad (3.7)$$
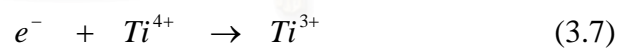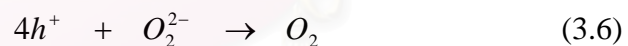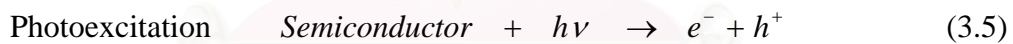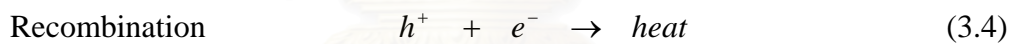
Electron-hole recombination processes may be suppressed by bulk and surface traps. In Figure 3.3, the energy levels of the bulk and surface traps fall within the band gap. The surface and bulk traps are localized, and the electrons trapped in such states are thus associated with a particular site on the surface or in the bulk of the solid. The population of bulk and surface traps depend on two factors, namely, the decrease in entropy that occurs
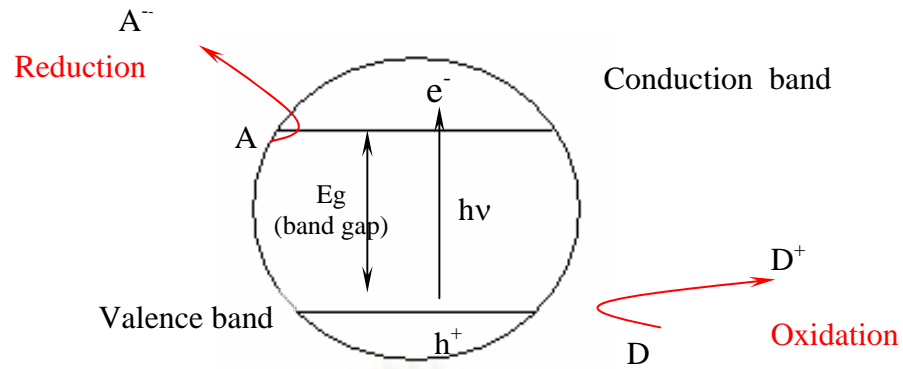
Figure 3.2 Photocatalytic process occurring on an illuminated semiconductor particle (Litter, 1999).

when electrons are trapped, and the difference in relative energy between the traps and the bottom of the conduction band.
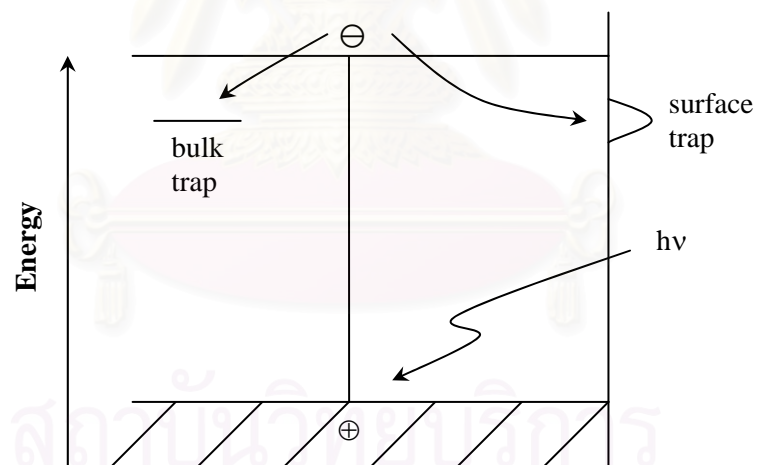
Figure 3.3 Surface and bulk electron trapping (Linsebigler *et al.*, 1995).

The photogenerated electrons reduce Ti (IV) cations to Ti (III) state, and the holes oxidize the O_2^{2-} anions. Then, oxygen atoms are ejected, creating oxygen vacancies (Fig. 3.4). Water molecules can then replace these oxygen vacancies producing chemisorbed hydroxyl groups (Fig.3.5a) these hydroxyl groups can

adsorb and spread water to create superhydrophilicity.(Fig 3.5b) The longer the surface is illuminated with UV light, the smaller the contact angle for water becomes; after about 30 min or so under a moderate intersity UV light source, the contact angle approaches zero, meaning that water has a tendency to spread perfectly across the surface.
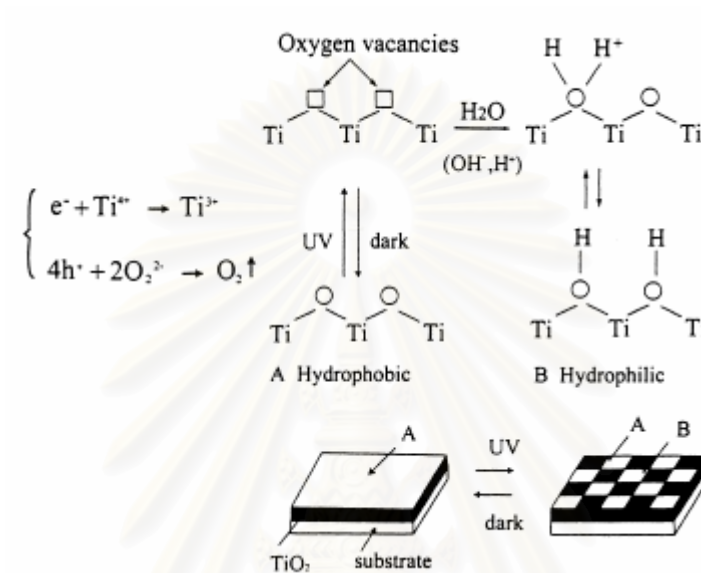
Figure 3.4 Mechanism of photo-induced hydrophilicity (Fujishima *et al.*, 2000)

OH OH OH OH OH OH OH OH OH   Chemisorbed OH
                                                          TiO$_2$ thin film

                                                          Substrate (glass)

a

OH   OH   OH   OH   OH   OH   OH   OH   OH   Physisorbed OH

OH   OH   OH   OH   OH   OH   OH   OH   OH   Chemisorbed OH
                                                             TiO$_2$ thin film

                                                             Substrate (glass)

b
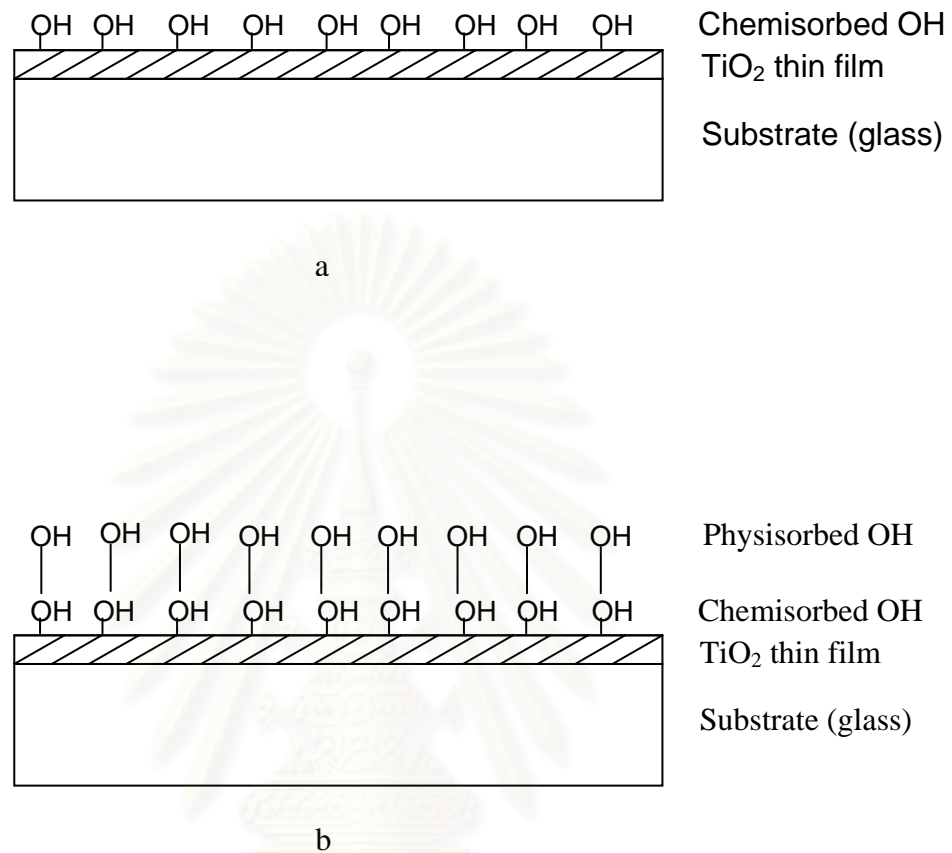
Figure 3.5 Mechanism of hydrophilic TiO$_2$ thin film. TiO$_2$ film illuminated by
UV light provides surface hydrophilic (a). Then, water can spread over
a film thoroughly (b).

3.4 Wettability and contact angle (De Gennes, 1985; Drew and Myers**)**

The contact angle is the angle at which a liquid/vapor interface meets
the solid surface. The contact angle is specific for any given system and is determined
by the interactions across the three interfaces. Most often the concept is illustrated
with a small liquid droplet resting on a flat horizontal solid surface (see Figure 3.6).
Ideally, the droplet should be as small as possible because the force of gravity, for
example, can actually change the above-mentioned angle. The shape of the droplet is
determined by Young equation in Equation (3.8).

$$\cos\theta \quad = \quad \frac{\sigma_{sa} - \sigma_{sl}}{\sigma_{la}} \qquad 3.8$$

Where θ = contact angle

σ_{sa} = surface tension between solid and ambient atmosphere

σ_{sl} = surface tension between solid and liquid

σ_{la} = surface tension between liquid and ambient atmosphere

The theoretical description of contact angle arises from the consideration of a thermodynamic equilibrium between the three phases: the liquid phase of the droplet (l), the solid phase of the substrate (s) and the gas/vapor phase of the ambient (a) (see Figure 3.6). At equilibrium, the chemical potential in the three phases should be equal. It is convenient to frame the discussion in terms of the interfacial energies or surface tension.
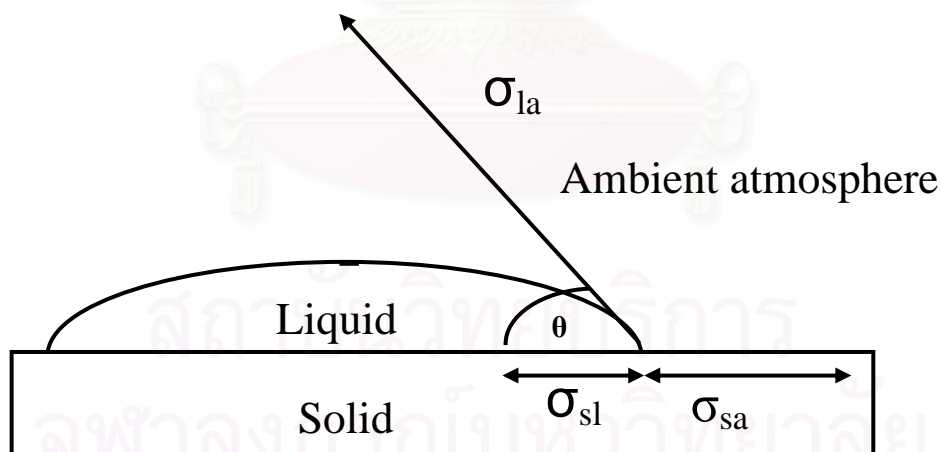
Figure 3.6 The force balance among the three surface tensions for determining the contact angle.

The wettability of substrate can be classified by the contact angle in 4 regions.

1. $\theta < 5^o$ Water can spread completely over the substrate surface. This state is called "superhydrophilic".
2. $5^o < \theta < 90^o$ The surface chemistry allows these materials to be wetted forming a water film or coating on their surface. This state is called "hydrophilic".
3. $90^o < \theta < 150^o$ Materials have little or no tendency to adsorb water and water tends to bead on their surfaces. This state is called "hydrophobic".
4. $\theta > 150^o$ Water droplets simply rest on the surface, without actually wetting to any significant extent. This state is called "superhydrophobic".

3.5 Film formation on substrate

Clear solution and film formation of titania depend on titanium concentration and pH of sol as show in phase diagram (See Figure 3.7). Each titania form has its boundary and regime in this diagram. Titania clear sol transform to film by rising concentration during coating process, water will evaporate to atmosphere. pH in the range of 2-4 makes positive charge titania surface and it bonds to surface substrate with electronic bonding. Furthermore, titania bond is tighten by sintering of titania during calcination process.

Figure 3.7 Total titanium concentration versus pH phase diagram drawn according to thermodynamics data. (Lencka *et at.,*1993)

CHAPTER IV

MATERIALS AND METHODS

4.1 Preparation of titanium dioxide thin films
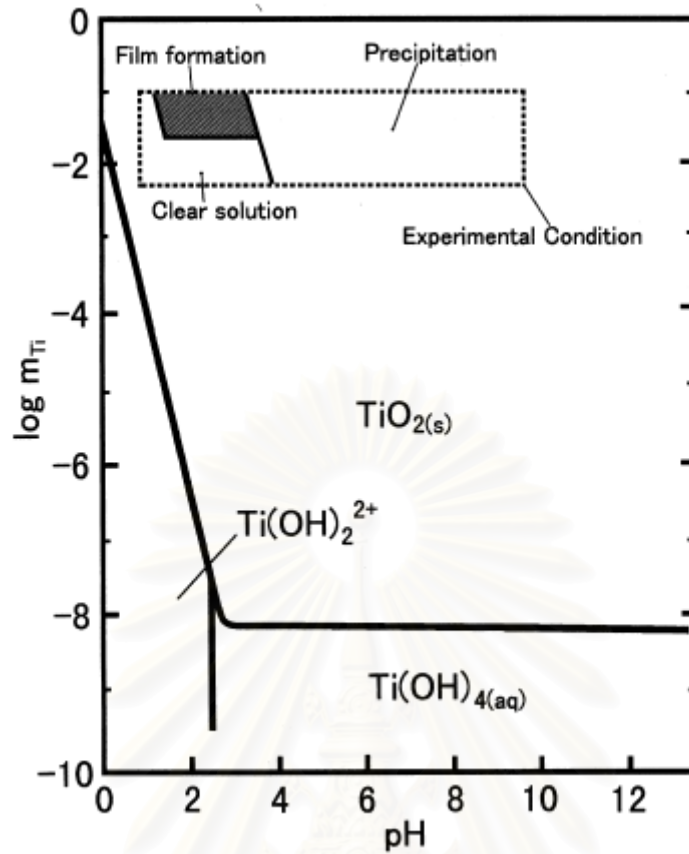
This section describes methods for preparation of titanium dioxide thin film using sol-gel processes.

4.1.1 Preparation of titanium dioxide

Titanium dioxide was prepared using a sol-gel method, and titanium isopropoxide (Aldrich Chemical, Milwaukee, WI) was employed as a precursor. First, 7.33 ml of 70% nitric acid (Asia Pacific Specialty Chemicals Limited) was added to 1000 ml of distilled water. While the acidic solution was stirred, 83.5 ml of titanium isopropoxide was added slowly. The suspensions were stirred continuously at room temperature for about 3 days until clear sol was obtained. After that, the sol was dialyzed in a cellulose membrane with a molecular weight cutoff of 3500 (Spectrum Companies, Gardena, CA). Prior to use, the dialysis tubing was washed in an aqueous solution of 0.001M EDTA and 2% sodium hydrogen carbonate. The wash solution was prepared by dissolving 0.372 grams of EDTA (Asia Pacific Specialty Chemicals Limited) and 43 grams of sodium hydrogen carbonate powder, 99.93% (Fisher Scientific Chemical) in one liter of distilled water. Dialysis tubing was cut into sections of 32 cm in length and was submerged in the wash solution. Then the membrane was heated to 80 °C and held there for 30 minutes while simultaneously being stirred. After the solution was cooled to room temperature, the tubing was again washed with distilled water. The tubing was again immersed in one liter of fresh distilled water while being stirred continuously, and was heated to 80°C. The tubing was rinsed one more time and was stored in distilled water at 4°C until needed. The clear sol was placed in dialysis tubing. Then the tubing containing the sol was submerged in distilled water using a ratio of 100 ml of sol per 700 ml of distilled

water. The water was changed daily for 3-4 days until the pH of the water reached 3.5 to remove solvents. The resulting product is dialyzed sol.

4.1.2 Preparation of titanium dioxide thin films

Thin film of titanium dioxide was prepared by a dip coating technique using in dialyzed titania sol. The substrate was clean glass slide (Menzel-Glaser). After coating, the sample was calcined under hydrogen, air and stack atmosphere at 350, 450, and 550 ^{o}C. Flow rates of air and hydrogen used for calcination were 5 l/h. The heating rate was 10 ^{o}C/min and holding time in the furnace was two hours.

4.2 Characterization of titanium dioxide thin film

In order to determine physical and chemical properties of thin films, various characterization techniques were employed. Such techniques are discussed in this section.

4.2.1 X-ray diffractomety (XRD)

XRD was employed to identify crystal phase and crystallinity of thin film. The equipment used was a SIEMENS D 5000 X-ray diffractometer with CuK$_{\alpha}$ radiation with Ni filter in the 2θ range of 20-60° with a resolution of 0.02^{o}. The sample, TiO$_2$ film on glass, was put in the XRD holder and run in the same manner as the other powder sample.

4.2.2 X-ray photoelectron spectroscopy (XPS)

XPS was determined quantity of Ti oxidation state and functional group, OH. The equipment was AMICUS XPS model with analyzer that operated at 20 mA and 12 kV. Mg anode used as X-ray photoelectron source. Etching mode was operated at 50 mA and 5 kV during Ar ion bombardment and analyzed with the same

condition above. The X-ray photoelectron spectra were referenced to the C 1s peak (285.00 eV).

4.3 Measurement of photo-induced hydrophilictiy of TiO_2

Photo-induced hydrophilicity of TiO_2 was determined in the term of contact angle measurement. Each TiO_2-coated glass was measured for initial contact angle value before irradiation with 15 W black light blue fluorescent bulbs. A water droplet was dropped from the syringe designed for controlling droplet volume. The volume of a water droplet was approximately 2.5 ml. A sample was placed on the base and raised to meet the syringe. When water was in contact with a sample, the camera captured the projection picture. A water contact angle was then calculated using trigonometry formula. All equipment and computer program was TANTEC. After that, the samples were exposed to UV light for various time; 10, 20, 30, 60, 120 and 180 minutes in the black box. After that each sample was drawn to measure a contact angle with a same method above.

CHAPTER V

RESULT AND DISCUSSION

5.1 Phase structures

The bulk crystalline phases of samples were determined using X-ray diffractometry (XRD). XRD patterns of TiO_2 samples calcined at 350°C, 450°C ,and 550°C for two hours under various calcination atmospheres were displayed in Figures 5.1, 5.2, and 5.3, respectively.

From the XRD patterns of titania calcined at 350°C (Figure 5.1), the dominant peak of anatase were observed at 2θ of about 25.2°, which corresponded to the index of (101) plane. The peaks corresponding to other planes of anatase phase could not be clearly identified because of the interference from signals from glass support. XRD peaks that belong to rutile phase were not detected at this temperature. Moreover, inspection of intensities of anatase peaks in the sample, which correlated with crystallinity of the sample, revealed that the sample calcined under hydrogen atmosphere possessed the lowest crystallinity when compared to the samples calcined under other conditions.
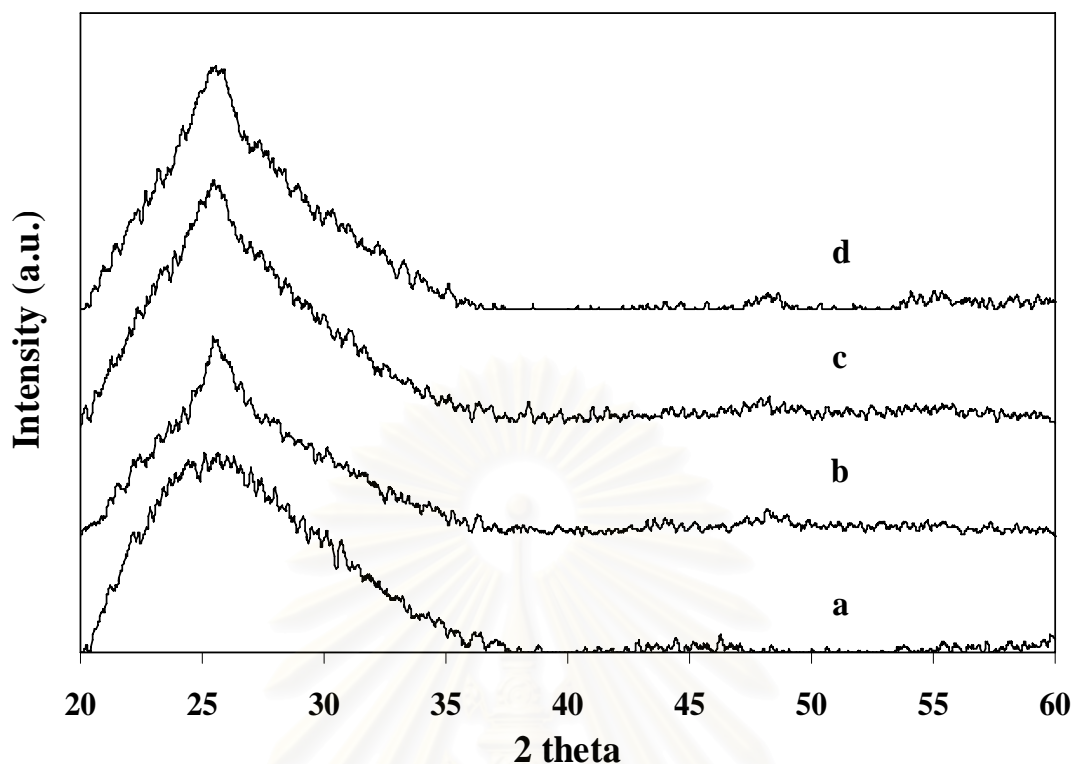
Figure 5.1 XRD patterns of TiO$_2$ film calcined at 350 ^{o}C under different atmospheres: air flow (b), hydrogen flow (c), and stagnant air (d). Cover glass was used as a blank (a).

When the films were calcined at 450 ^{o}C (see Figure 5.2), a peak corresponded to (110) plane of rutile phase appeared at 2θ of about 27.4°. All samples were the combination of anatase and rutile phases. Rutile content in the films grew larger when as calcination temperature was increased as the peak corresponded to rutile phase became more pronounced for the samples calcined at 550 ^{o}C (see Figure 5.3). At this temperature, the sample calcined under hydrogen atmosphere was reduced so XRD pattern displayed the low peak intensity as a result of low crystallinity or high bulk defects for the film (Rekoske *et al.,* 1996). Moreover, titania crystallite size grew larger as calcinations temperature was increased. However, under hydrogen calcinations, crystallite size did not change clearly (see Table 5.1).

Table 5.1 Summary of crystallite size of TiO_2 under various calcination conditions obtained by XRD analysis.

Atmosphere	Calcination temperature (^{o}C)	Crystallite size (nm)	
		Anatase	Rutile
Air	350	7.3	n/a
	450	8.1	12.8
	550	10.6	18.9
Stagnant air	350	7.6	n/a
	450	8.7	27
	550	12.5	21.1
Hydrogen	350	7.5	n/a
	450	8	24.9
	550	8	13

Figure 5.2 XRD patterns of TiO_2 film calcined at 450 ^{o}C under different atmospheres: air flow (b), hydrogen flow (c), and stagnant air (d). Cover glass was used as a blank (a).

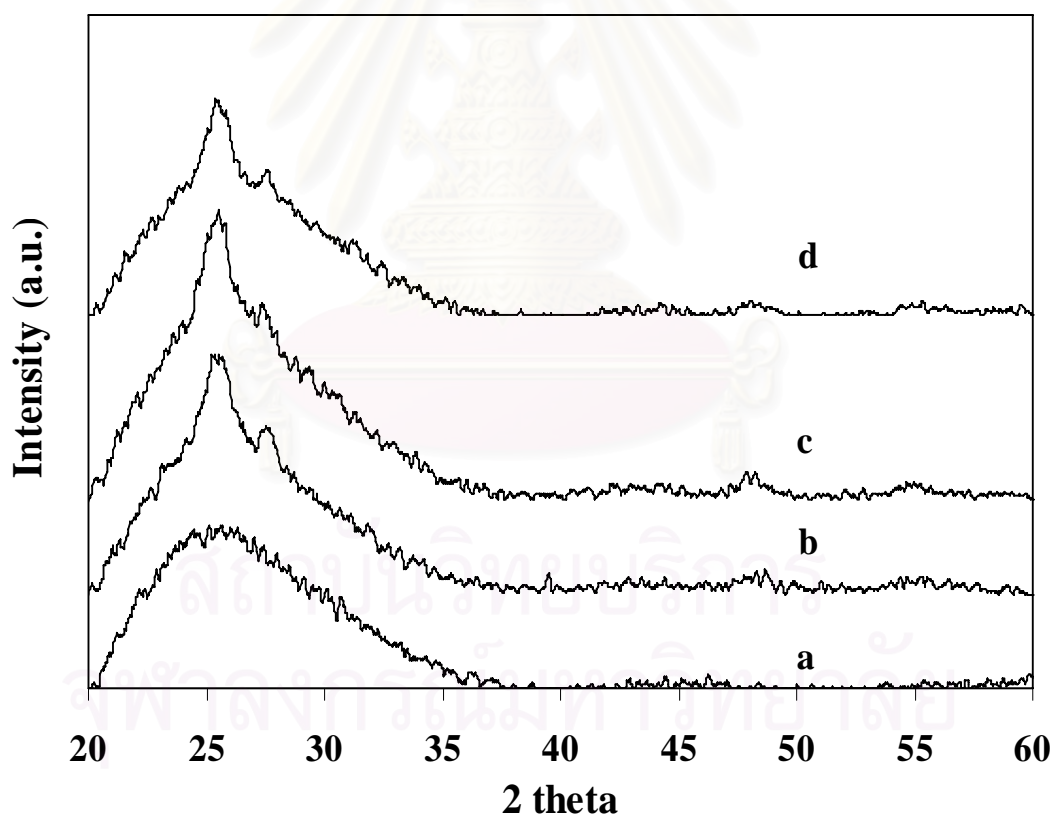**Figure 5.3** XRD patterns of TiO_2 film calcined at 550 ^{o}C under different atmospheres:
air flow (b), hydrogen flow (c), and stagnant air (d). Cover glass was used
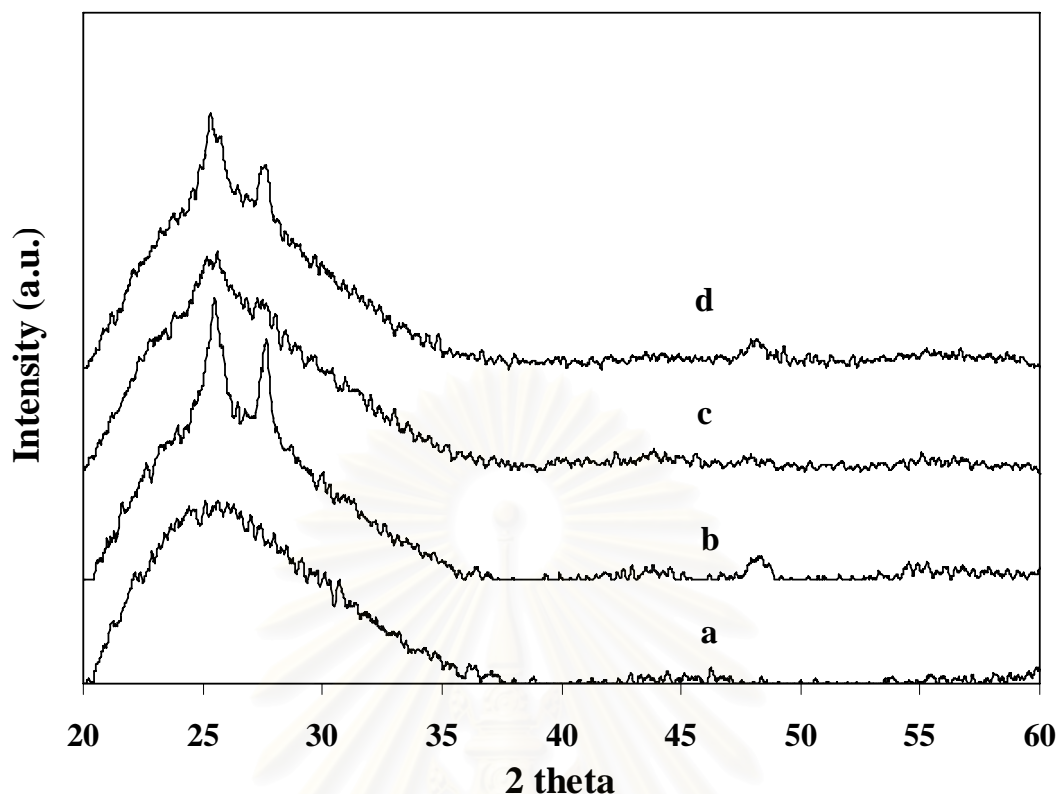as a blank (a).

For the two-step calcinations process, TiO_2 film was first calcined
under air flow at 450 ^{o}C and was then calcined under stagnant air at 350°C (condition
1), under hydrogen flow at 350 ^{o}C (condition 2) and calcined under air and hydrogen
flow at 350 ^{o}C and 450 ^{o}C respectively (condition 3). The holding time for all
conditions was 2 hr. For the first two conditions, the calcination temperature in the
second step was lower than the first step so XRD patterns remained unchanged (see
Figure 5.4). However, for condition 3, the higher calcination temperature in the
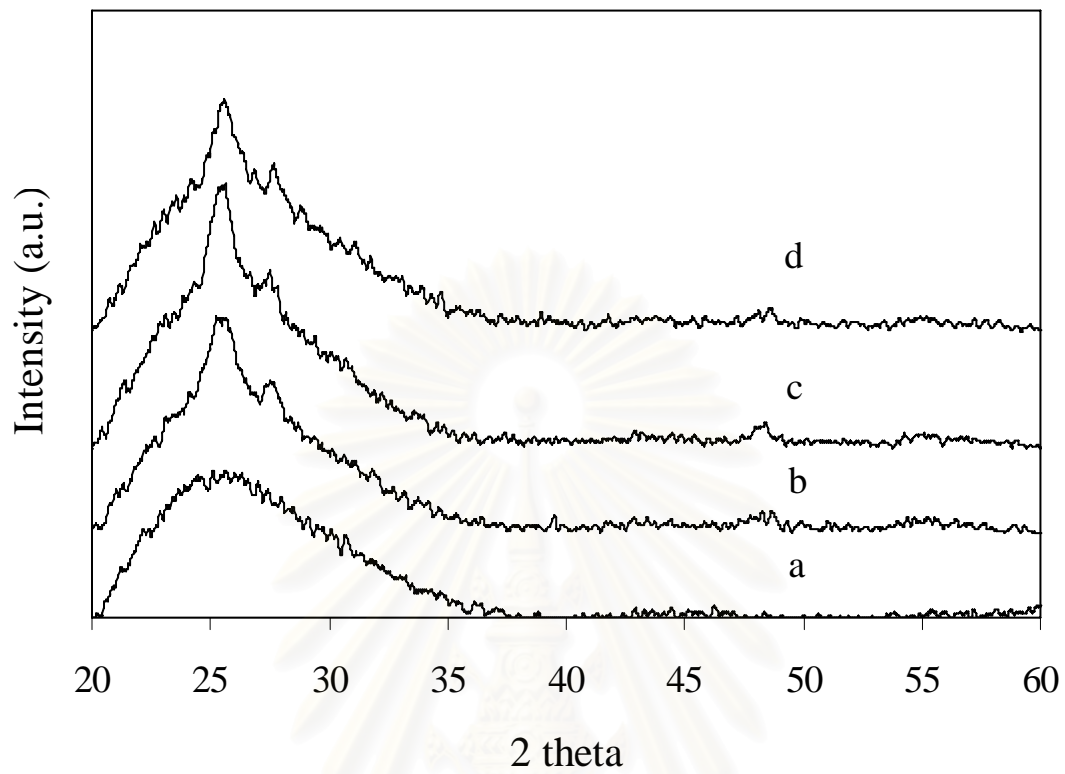second step brought about the formation of more rutile phase.

Figure 5.4 XRD patterns of TiO$_2$ films calcined in condition 1 (b), condition 2 (c), and, under air flow at 450 $^{\circ}$C (d). Cover glass was used as a blank (a).
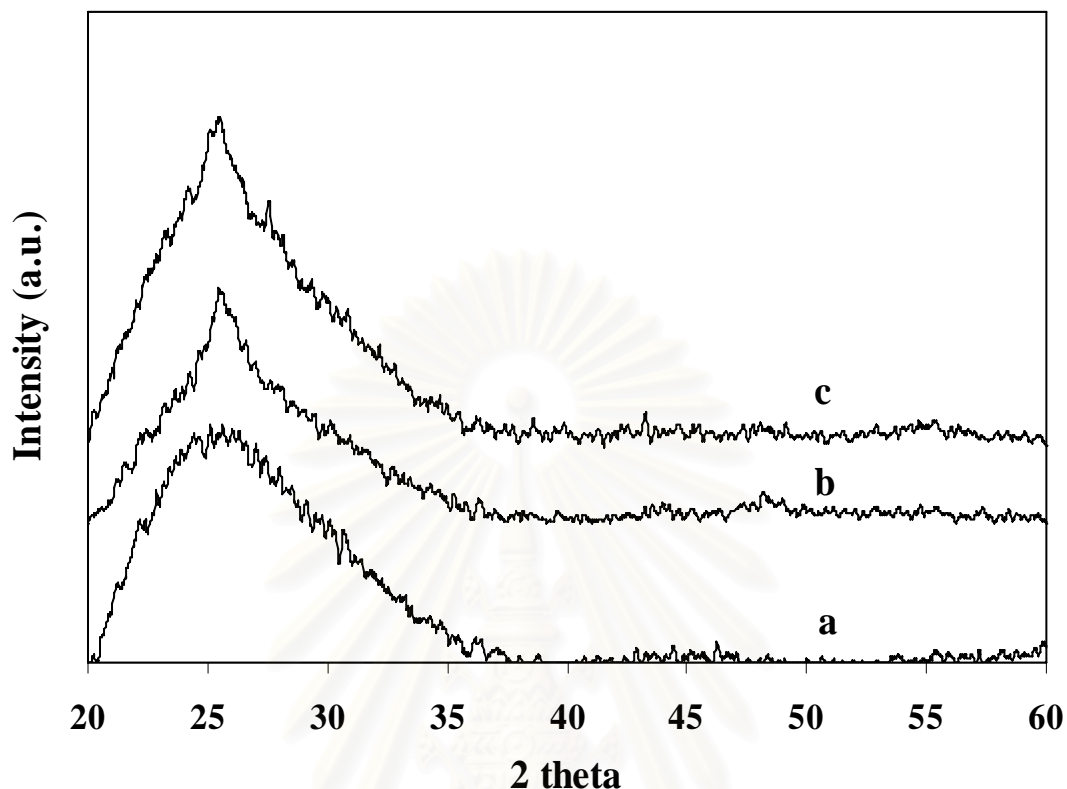
Figure 5.5 XRD patterns of TiO$_2$ films calcined in condition 3 (b) and under air flow
at 350 ^{o}C(c). Cover glass was used as a blank (a).

5.2 Oxidation state of titanium dioxide

Elemental components present in TiO$_2$ thin films could be determining
using X-ray photoelectron spectroscopy (XPS). Figure 5.6 displays a survey graph of
TiO$_2$ surface obtained from XPS. The major components were titanium and oxygen.
However, other element such as silicon was also detected. The signal of silicon was
attributed to glass substrate used as a support for the film.

Figure 5.6 Survey graph of components on TiO_2 surface.

O 1s peak was observed at a binding energy of ca. 531 eV, which corresponded to the main peak for oxygen in TiO_2. The other peaks for oxygen were oxygen from surface hydroxyl group and from water.
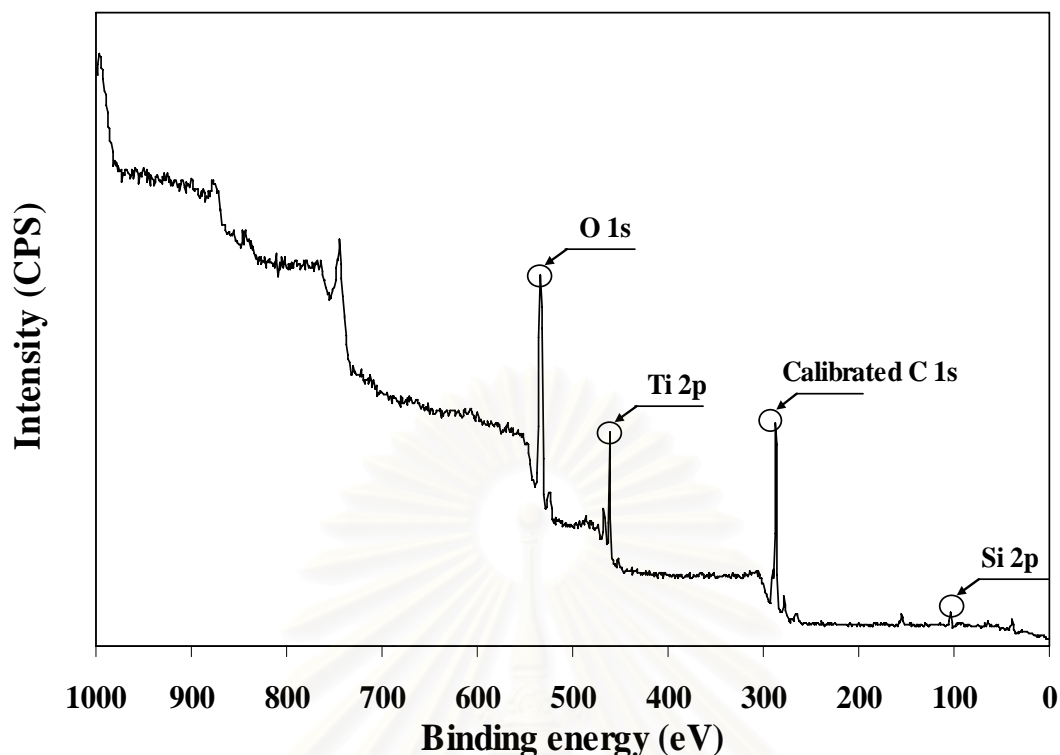
Ti 2p had two main peaks from Ti $2p_{3/2}$ and $2p_{1/2}$ orbital at binding energy of ca. 460 and 465.7 eV respectively. These two peaks corresponded to $Ti4^+$. Other oxidation state of titanium was not detected because $Ti3^+$ sites on the surface were adsorbed by hydroxyl group from the atmosphere. Etching mode was employed to remove hydroxyl group from TiO_2 surface. Argon ion bombarded the surface to peel off the outer most layer and reveal Ti^{3+} in TiO_2 sample. Normally, the higher the oxidation state of an element, the higher the binding energy. The position of binding energy of each oxidation state of titanium and reference were listed in Table A.1

Table 5.1 Summary of Ti^{3+}/Ti^{4+} ratio from XPS measurements for titania films at various calcination conditions.

Calcination Condition		Ti^{3+}/Ti^{4+} ratio
Atmosphere	Temperature (^{o}C)	
Air	350	0.789
	450	0.899
	550	0.915
Hydrogen	350	0.918
	450	0.932
	550	1.091
Stagnant air	350	0.922
	450	1.009
	550	0.955
Air/Stagnant air*	450/350	1.104
Air/Hydrogen*	450/350	1.160
Air/Hydrogen*	350/450	1.220

* : The condition involved calcination in two steps.

Table 5.1 summarizes ratios of Ti^{3+} content to Ti^{4+} content for various titania film.From the table, Ti^{3+} content compared to Ti^{4+} increased when calcination temperature was increased. Titania films that were calcined under air flow had the lowest Ti^{3+} contents while calcination under stagnant air brought about the highest values of Ti^{3+} content for titania films. However, at the temperature above 500 ^{o}C calcination under hydrogen atmosphere produced more Ti^{3+} than calcination under stagnant air as a result of reduction by hydrogen. Inspection of Table 5.1 revealedthat calcination atmosphere had greater effect on Ti^{3+} content that calcination temperature. Furthermore, the two-step calcinations process gave rise to similar Ti^{3+} content for all three conditions. Comparing to the one-step calcination process, the two-step process produced higher Ti^{3+} content for titania films.

5. 3 Photo-induced hydrophilicity

Under UV irradiation, the contact angle of TiO_2 thin film gradually decreased until the angle reached a steady value, call "saturated contact angle". So irradiation with UV light improved hydrophilic property of TiO_2 film.

The results from contact angle measurements for various TiO_2 films that were calcined under stagnant air, hydrogen flow, and air flow are presented in Figures 5.7, 5.8, and 5.9, respectively. The contact angles of TiO_2 calcined under stagnant air and hydrogen flow reached saturated values after 30 minutes of UV irradiation (see Figures 5.7 and 5.8). As the calcination temperature was increased, the saturated contact angel of titania film was smaller, that is, the film became more hydrophilic. This trend was also observed for titania films that were calcined under air flow. The decrease in saturated contact angle, or increase in hydrophilicity, of the samples was attributed to higher Ti^{3+} content and the presence of rutile phase.

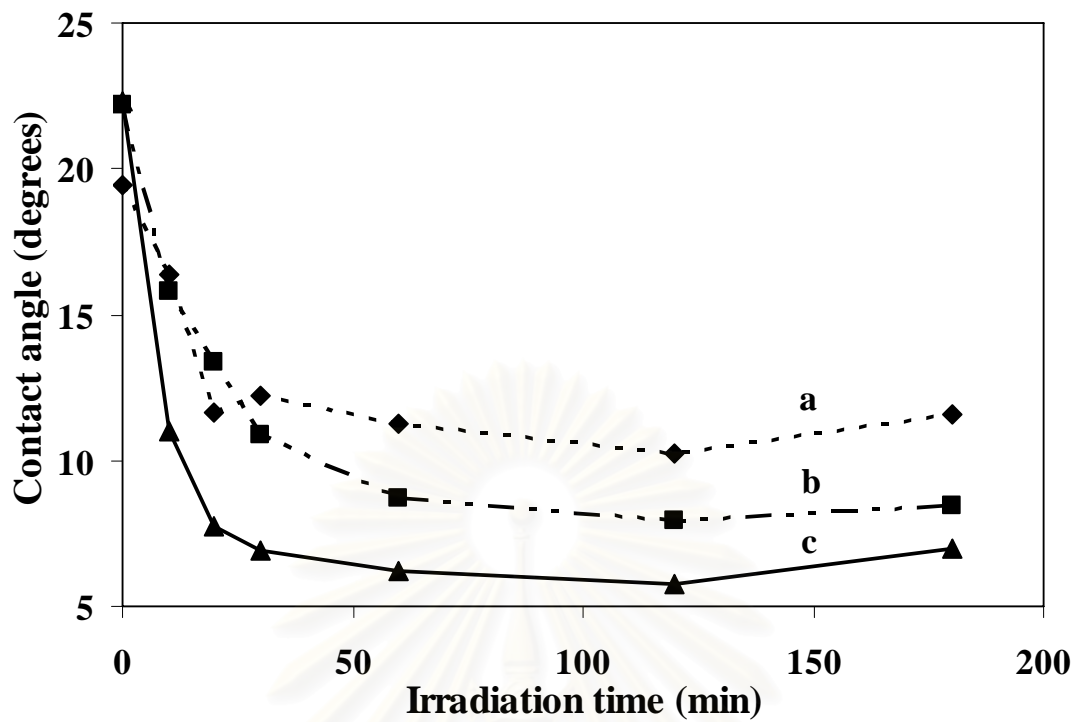**Figure 5.7** Contact angle of TiO_2 thin film calcined under stagnant air at 350 ^{o}C (a), 450 ^{o}C (b) and 550 ^{o}C (c).
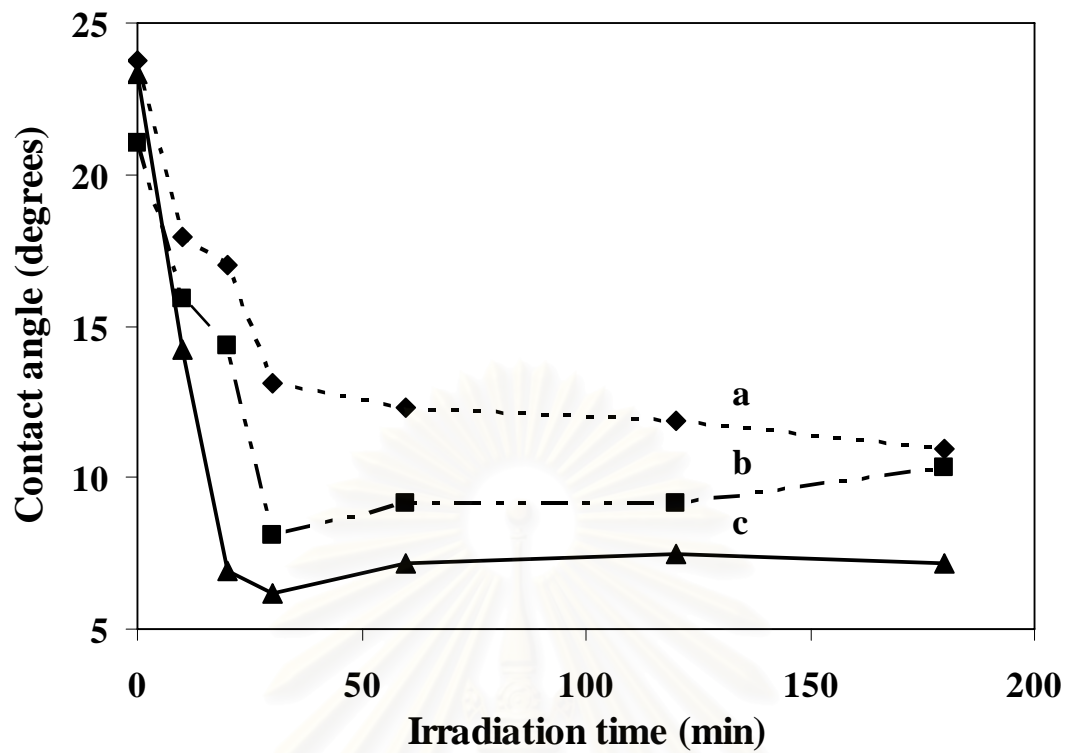
Figure 5.8 Contact angle of TiO$_2$ thin film calcined under hydrogen at 350 ^{o}C (a), 450 ^{o}C (b) and 550 ^{o}C (c).
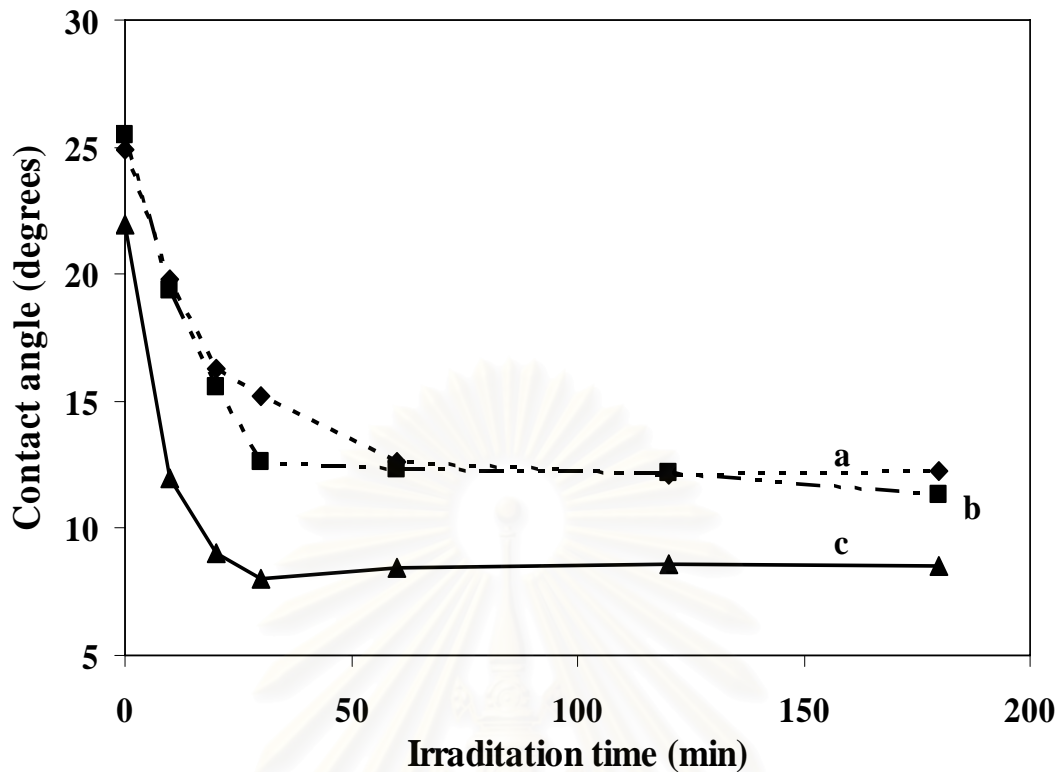
Figure 5.9 Contact angle of TiO_2 thin films calcined under air flow at 350 ^{o}C (a), 450 ^{o}C (b) and 550 ^{o}C (c).

Figure 5.10, 5.11, and 5.12 display contact angle of TiO_2 thin films that were calcined under various atmosphere at 350 ^{o}C, 450 ^{o}C, and 550 ^{o}C, respectively.The saturated contact angle of TiO_2 films calcined under air flow was the highest while this value was the lowest for the films calcined under stagnant air. The difference in saturated contact angles was attributed to amount of Ti^{3+} defects. This parameter was influenced by calcination atmosphere. Under sufficient air flow rate the combustion of residual organic introduced by molecular precursors was complete under sufficient air flow rate. However, if available oxygen during calcination calcining was insufficient, oxygen molecule from titania structure was consumed to burn this residual organic instead (Yu *et al.,* 2000). This process led to titanium in TiO_2 being reduced from Ti^{4+} to Ti^{3+}
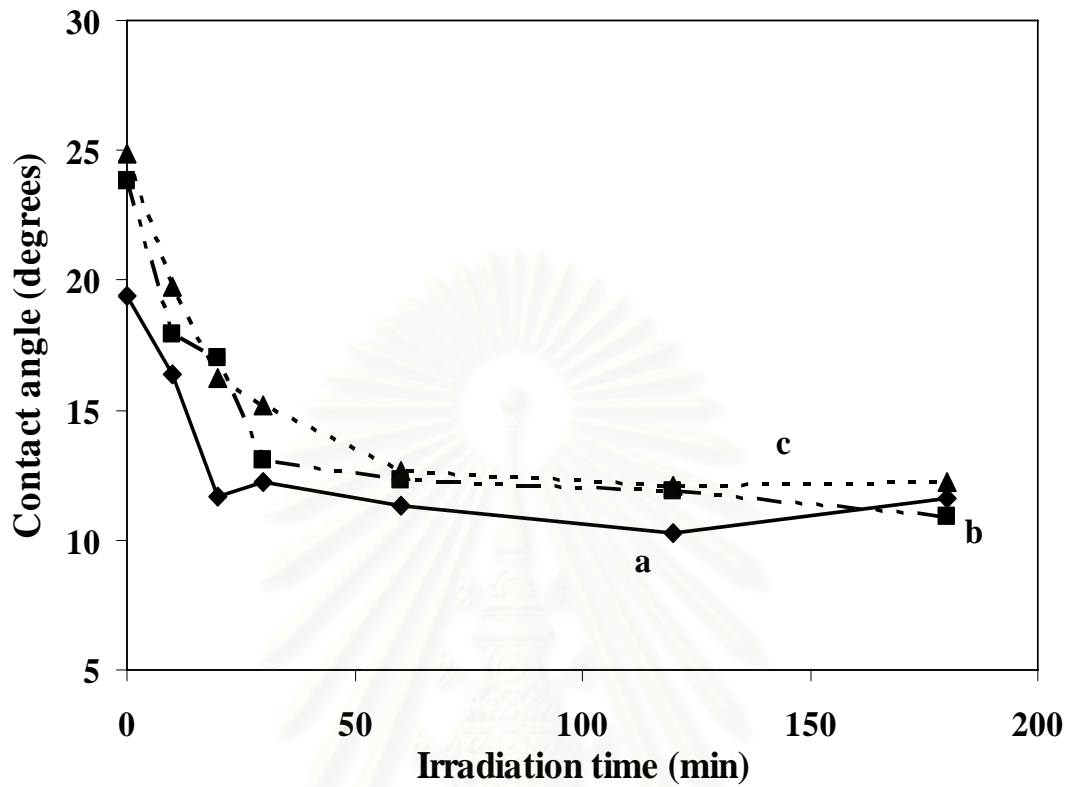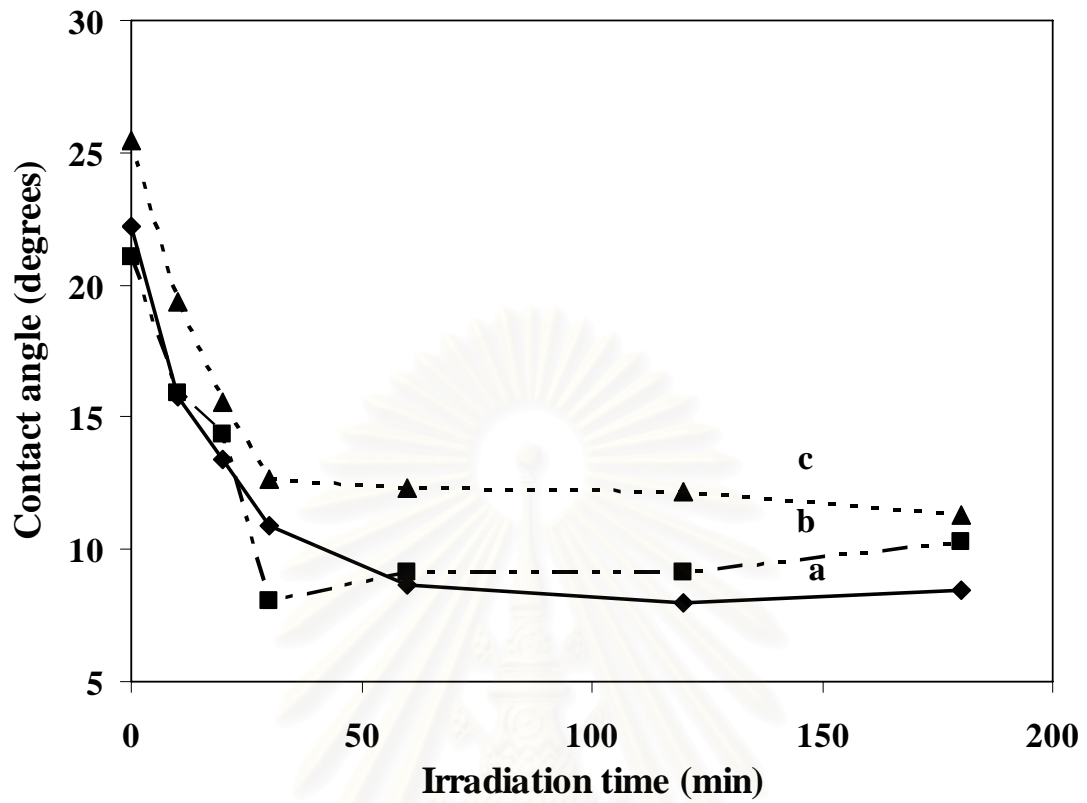
Figure 5.10 Contact angle of TiO_2 thin films calcined at 350 °C under stagnant air (a),

hydrogen flow (b) and air flow (c).

Figure 5.11 Contact angle of TiO$_2$ thin films calcined at 450 $^{\circ}$C under stagnant air (a), hydrogen flow (b) and air flow (c).
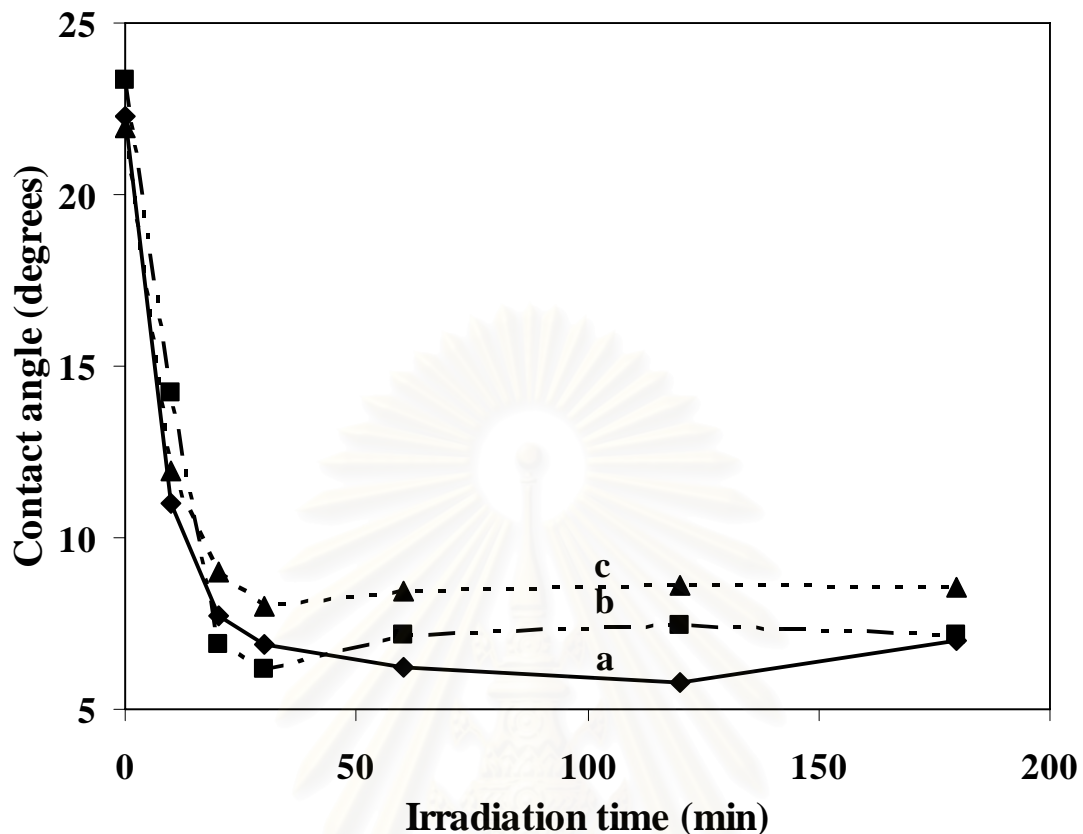
Figure 5.12 Contact angle of TiO$_2$ thin films calcined at 550 $^{\circ}$C under stagnant air (a),
hydrogen flow (b) and air flow (c).

Calcination under hydrogen flow produced more Ti^{3+}surface defects
for TiO$_2$ (Sekiya *et al.,* 2001; Liu *et al.,* 2002). However, this calcination process
failed to produce TiO$_2$ films with the lowest saturated contact angle. Therefore, Ti^{3+}
srufece defect was only one of the factors that had and effect on saturated contact
angle of the samples. Other factors included crystallinity of TiO$_2$ and bulk defects in
the film.

The results of contact angle measurements for TiO$_2$ films that
underwent the two-step calcination processes are displayed in Figure 5.13. By fixing
the condition in the first calcination step (450 $^{\circ}$C under air flow), the bulk defects,
content in the films was controlled to be similar. The second calcination step would

produce different amount of Ti^{3+} surface defects because of different calcination atmosphere employed.

The saturated contact angles of TiO$_2$ films that underwent the two-step calcination process were lower that that of TiO$_2$ films that underwent the one-step calcination. This finding was attributed to formation of more Ti^{3+} surface defects during the second calcination step (Lu *et al.,* 1994; Rekoske *et al.,* 1997; Guillemot *et al.,* 2002) , there by lowering the saturated contact angle of the samples. The saturated contact angle of TiO$_2$ film that was calcined under hydrogen films in the second calcination step was smaller than that of the film that was calcined under stagnant air in the second step because more Ti^{3+} defects were produced when the film was calcined under hydrogen flow.
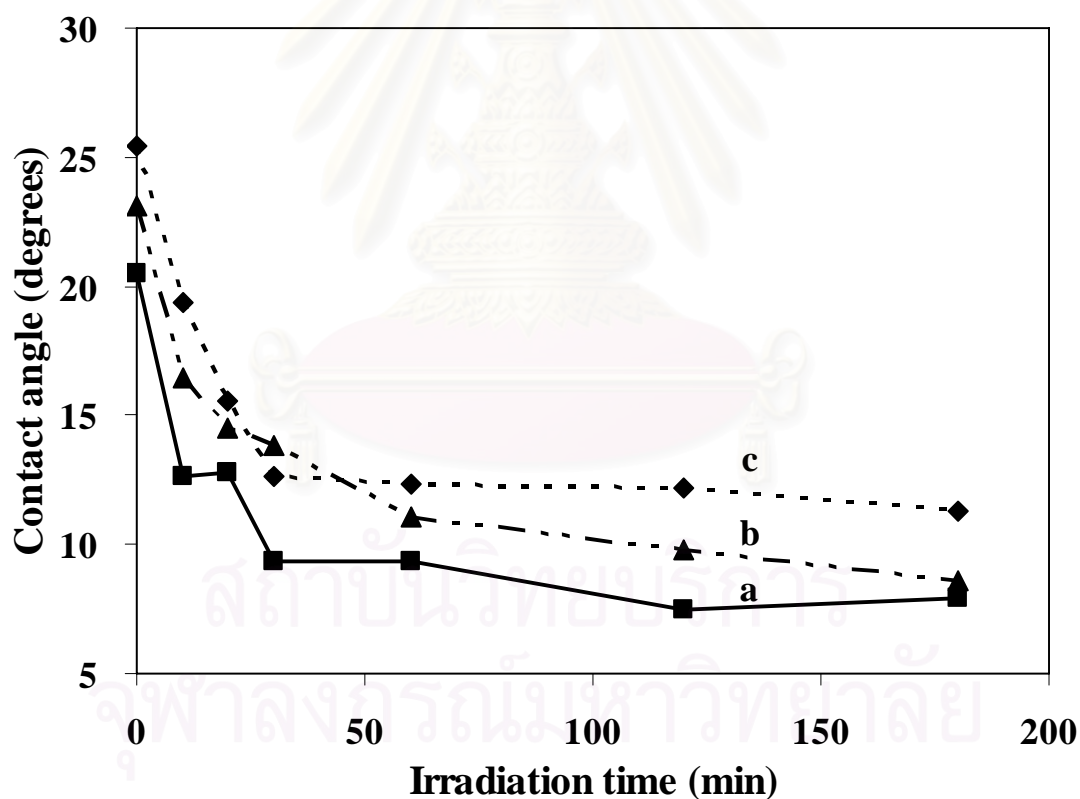
Figure 5.13 Contact angle of TiO$_2$ thin films calcined at 450 ^{o} C under air flow and 350 ^{o} C under hydrogen flow (a), at 450 ^{o} C under air flow and 350 ^{o} C under stagnant air (b), and at 450 ^{o} C under air flow (c).
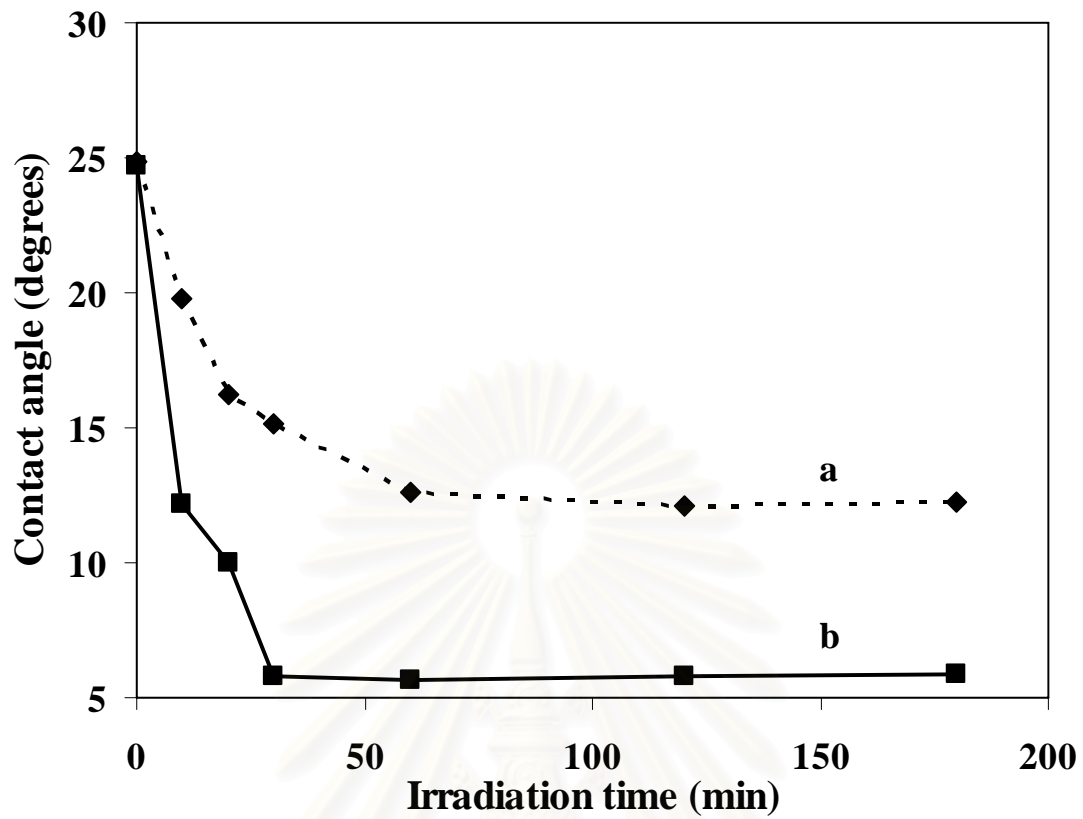
Figure 5.14 Contact angle of TiO_2 thin films calcined at 350 ^{o} C under air flow and
450 ^{o} C under hydrogen flow (a) and at 350 ^{o} C under air flow (b).
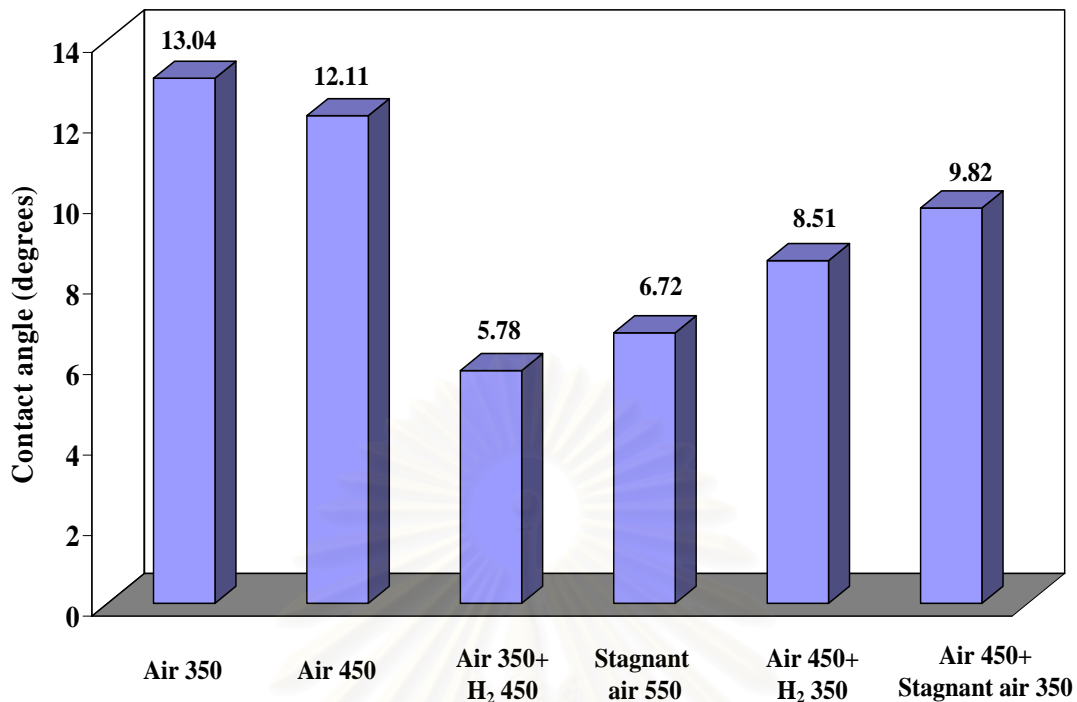
Figure 5.15 Comparison the saturated contact angle calcined in various conditions.
Two-step calcination process made the film had lower contact angle.

The limitation of calcination was thermal stability of glass substrate which was damaged at temperature above 600 ^{o}C so using two-step calcination process could improve hydrophilicity. Figure 5.15 displays the saturated contact angle of titania films that could be lowered by two-step calcination process. Moreover, calcination temperature of two-step calcination process (350 ^{o}C and 450 ^{o}C) was lower but provided the higher hydrophilic than one-step calcination process (550 ^{o}C).

CHAPTER VI

CONCLUSIONS AND RECOMMENDATIONS FOR FUTURE RESEARCH

This chapter summarizes experimental results involving characterization of titania thin films for studies of the photo-induced hydrophilicity. Recommendations for future research are also presented.

6.1 Conclusions

1. The hydrophilic property of TiO_2 thin films was controlled by Ti^{3+} surface defect. The defect content increased with the increasing of calcination temperature and calcination atmosphere as well as rutile content.

2. Regarding calcination atmosphere, the smallest saturated contact angle was observed in the sample that was calcined under stagnant air probably due to the highest Ti^{3+} surface defect.

3. The two-step calcination process provided smaller saturated contact angle than the one-step calcination process even at a lower calcination temperature. The first step transformed titania structure from amorphous to crystals while the second step created more Ti^{3+} surface defect.

6.2 Recommendations for future research

1. The slide glass melts at temperature above 600 ^{o}C so it is limit for the experiment. The substrate should be change to the thermalstability material such quartz or metal to study effect of temperature to the other properties.

2. The other parameter that may control hydrophilic property of titania thin films, namely, morphology or specific area should be study too.

3. The interesting variables that influence to the parameter, namely, heating rate of calcination , doped metal or holding should be varied.

REFERENCES

De Gennes, P.G. Wetting: statics and dynamics. Reviews of Modern Physics 57,3
  (part I), July 1985, 827-823.

Drew and Myers, Wirely VCH. Surfaces, Interfaces, and Colloids Principles and
  Applications second edition.

Fu, X., Clark L., Zeltner W., and Anderson A. Effects of reaction temperature and
  water vapor content on the heterogeneous photocatalytic oxidation of ethylene.
  Journal Photochemistry and Photobiology. A: Chemistry. 97 (1996): 181-186.

Fujishima, A., Hashimoto, K., and Watanabe, T., TiO_2 photocatalysis: fundamental
  and applications. 1 st ed. Tokyo: BKC, 1999.

Fujishima, A., Rao T.N. and Tryk, D.A. Titanium dioxide photocatalysis. Journal of
  Photochemistry and Photobiology C: Photochemistry Reviews 1 (2000): 1-21.

Gao, Y., Masuda, Y. and Koumoto, K. Light-excited superhydrophilicity of
  amorphous TiO_2 thin films deposited in an aqueous peroxotitanate solution.
  Langmuir 20 (2004): 3188-3194.

Guillemot, F., Porte, M.C., Labrugere, C. and Baquey, Ch. Ti^{4+} to Ti^{3+} conversion of
  TiO_2 uppermost layer by low-temperature vacuum annealing: interest for
  titanium biomedical applications. Journal of Colloid and Interface Science 255
  (2002): 75-78.

Lee, Y.C., Hong, Y.P., Lee, H.Y., Kim, H., Jung, Y.J., Ko, K.H., Jung, H.S. and
  Hong, K.S. Photocatalysis and hydrophilicity of doped TiO_2 thin films.
  Journal of Colloid and Interface Science 267 (2003): 127-131.

Lencka, M.M. and Riman, R.E. Thermodynamic modeling of hydrothermal synthesis
  of ceramic powders Chemistry Material 5 (1993) 61.

Linsebigler, A. L., Lu, G. and Yates, Jr. J. T. Photocatalysis on TiO_2 surfaces: principles, mechanism, and selected results. Chemistry Review 95 (1995): 735-758.

Litter, M.L. Heterogeneous photocatalysis transition metal ions in photocatalytic systems. Applied Catalysis B: Environment 23 (1999): 89-114.

Liu, H., Ma, H.T., Li, X.Z., Li, W.Z., Wu, M. and Bao, X.H. The enhancement of TiO_2 photocatalytic activity by hydrogen thermal treatment. Chemosphere 50 (2003): 39-46.

Lu, G., Linsebigler, A. and Yates, J.T.Jr. Ti^{3+} defect sites on chemical detection of active sites. Journal of Physical Chemistry 98 (1994): 11733-11738.

Othmer, K. Encyclopedia of chemical technology. Vol. 6. 4 th ed. New York: A Wiley-Interscience Publication, John Wiley&Son, 1991.

Rekoske, J.E. and Barteau, M.A. Isothermal reduction kinetics of titanium dioxide-based materials. Journal of Physical Chemistry B 101 (1997): 1113-1124.

Sekiya, T., Yagisawa, T. and Kurita, S. Annealing of anatase titanium dioxide under hydrogen atmosphere. Journal of the Ceramic Society of Japan. 109 (2001): 672-675.

Su, C., Hong, B., and Tseng, C. Sol-gel preparation and photocatalysis of titanium dioxide. Catalysis Today. 96 (2004): 119-126.

Suriye, K., Praserthdam, P. and Jongsomjit, B. Impact of Ti^{3+} present in titania on characteristics and catalytic properties of the Co/TiO_2 catalyst. Industrial and Engineering Chemistry Research 44 (2005): 6599-6604.

Trapalis, Ch., Kozhykharov, V., Samuneva, B. and Stafanov, P. Sol-gel processing of titanium-containing thin coatings, Part I. Preparation and structure. Journal of Material Science 28 (1993): 2352-2360.

Watanabe, T., Nakajima, A., Wang, R., Minabe, M., Koizumi, S., Fujishima, A. and Hashimoto, K. Photocatalytic activity and photoinduced hydrophilicity of titanium dioxide coated glass. Thin Solid Films 351 (1999): 260-263.

Yu, J. and Zhao, X. Effect of surface treatment on the photocatalytic activity and hydrophilic property of the sol-gel derived TiO_2 thin films. Materials Research Bulletin 36 (2001a): 97-107

Yu, J. and Zhao, X. Effect of surface microstructure on the super-hydrophilic property of the sol-gel derived porous TiO_2 thin films. Journal of Materials Science Letter 20 (2001b): 671-673.

Yu, J.C., Yu, J., Ho, W. and Zhoa, J. Light-induced super-hydrophilicity and photocatalytic activity of mesoporous TiO_2 thin films. Journal of Photochemistry and Photobiology A: Chemistry 148 (2002): 331-339.

Yu, J.G., Zhao, X.J., Du, J. Ch., Chen, M. and Chen, M. Journal of Sol-Gel. Science Technology 17 (2000): 163.
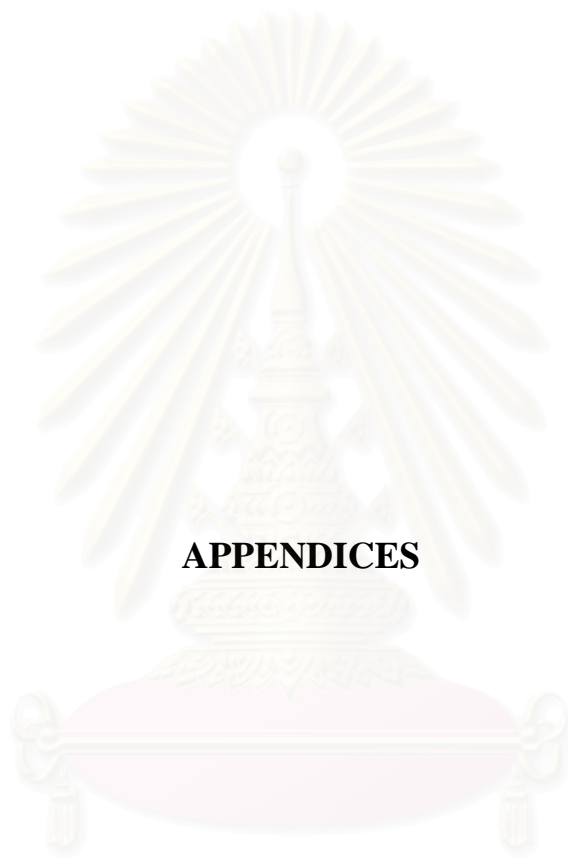
APPENDICES

APPENDIX A

CALCULATION OF THE CRYSTALLITE SIZE

Calculation of the crystallite size by Debye-Scherrer equation

The crystallite size was calculated from the width at half-height of the diffraction peak of XRD pattern using the Debye-Scherrer equation.

From Scherrer equation:

$$D = \frac{K\lambda}{\beta \cos \theta} \qquad (A.1)$$

where D = Crystallite size, Å

K = Crystallite-shape factor = 0.9

λ = X-ray wavelength, 1.5418 Å for CuKα

θ = Observed peak angle, degree

β = X-ray diffraction broadening, radian

The X-ray diffraction broadening (β) is the pure width of a powder diffraction, free of all broadening due to the experimental equipment. Standard α-alumina is used to observe the instrumental broadening since its crystallite size is larger than 2000 Å. The X-ray diffraction broadening (β) can be obtained by using Warren's formula.

From Warren's formula:

$$\beta^2 = B_M^2 - B_S^2 \qquad (A.2)$$

$$\beta = \sqrt{B_M^2 - B_S^2}$$

Where B_M = The measured peak width in radians at half peak height.

B_S = The corresponding width of a standard material.

Example: Calculation of the crystallite size of titania

The half-height width of 101 diffraction peak　　=　0.93125°

　　　　　　　　　　　　　　　　　　　　　　=　0.01625 radian

The corresponding half-height width of peak of α-alumina　=　0.004 radian

The pure width　　　=　$\sqrt{B_M^2 - B_S^2}$

　　　　　　　　　=　$\sqrt{0.01625^2 - 0.004^2}$

　　　　　　　　　=　0.01577 radian

β　=　0.01577 radian

2θ　=　25.56°

θ　=　12.78°

λ　=　1.5418 Å

The crystallite size　=　$\dfrac{0.9 \times 1.5418}{0.01577 \ \cos 12.78}$　=　90.15Å
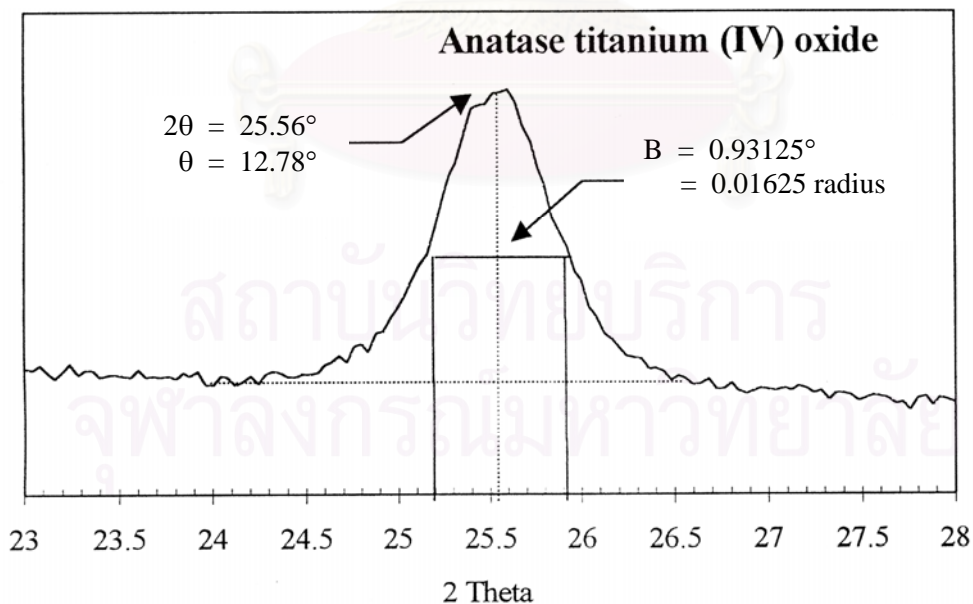
　　　　　　　　　　=　9 nm

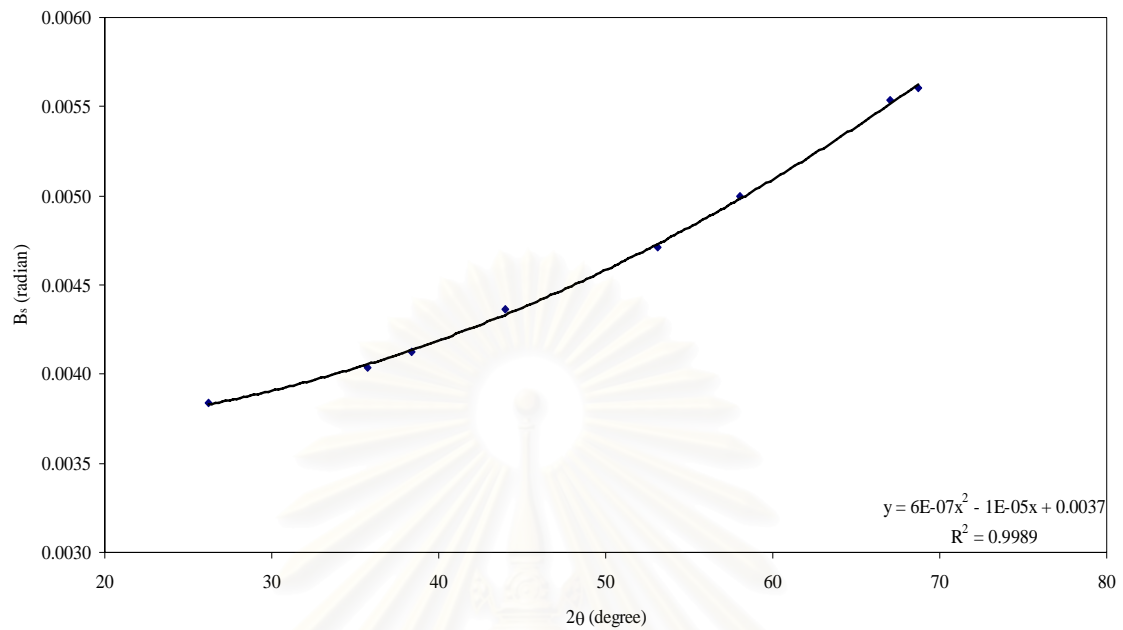**Figure A.1** The 101 diffraction peak of titania for calculation of the crystallite size

Figure A.2 The plot indicating the value of line broadening due to the equipment. The

data were obtained by using α-alumina as standard.

APPENDIX B

CALCULATION OF THE CONTACT ANGLE

The contact angle of sample was calculated from height and radius of water droplet using trigonometry formula.
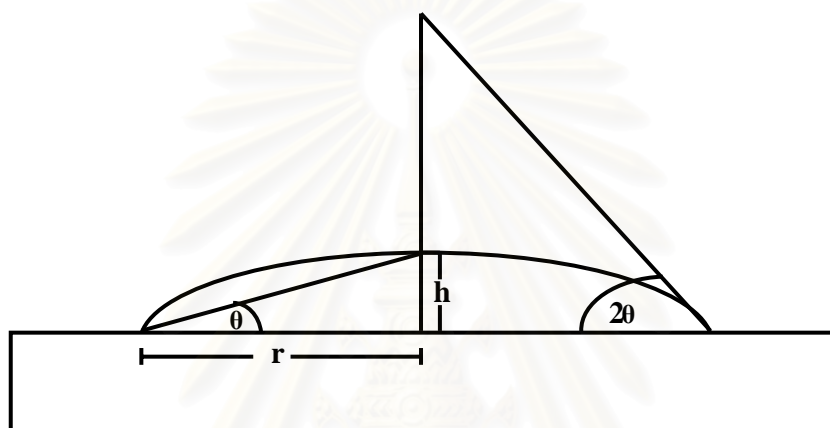

Figure B.1 The shape and dimension of water droplet on the substrate.

$$Contact\ angle \quad = \quad 2\arctan\frac{h}{r} \tag{B.1}$$

Where h = water droplet height

r = water droplet radius

2θ = Contact angle

APPENDIX C

POSITION OF TITANIUM OXIDATION STATE

The content of each Ti oxidation state can determine from the component area (see Figure C.1) and each binding energy position is list in Table C.1
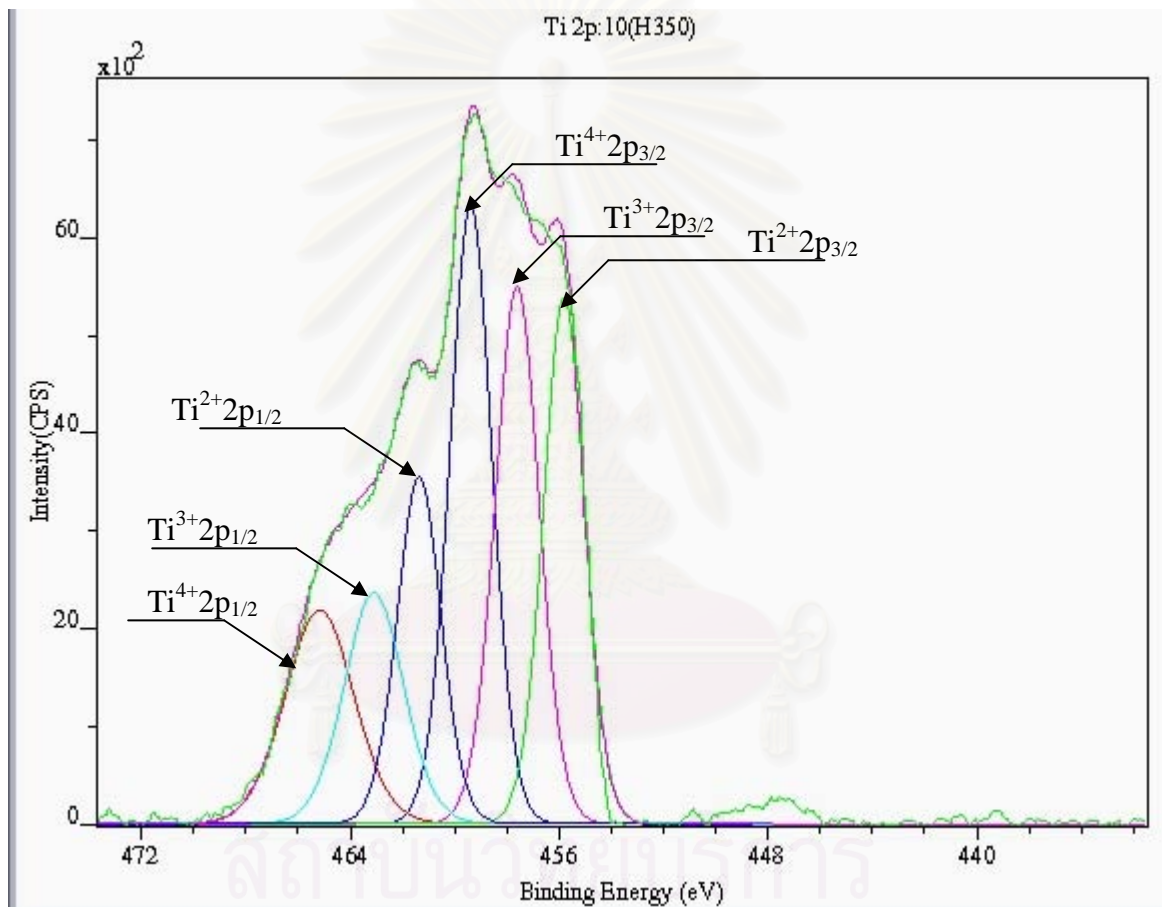

Figure C.1 The binding energy and area of each Ti oxidation state.

Table C.1 The list of binding energy position and reference of each element.

Element	Binding energy	Component	References.
O 1s	528.300	TiO	P.Madhu Kumar, Thin Films,2000
O 1s	531.100	Ti_2O_3	P.Madhu Kumar, Thin Films,2000
O 1s	530.100	TiO_2	P.Madhu Kumar, Thin Films,2000
O 1s	532.300	$(OH)^-$	P.Madhu Kumar, Thin Films,2000
O 1s	529.400	$(OH)^-$	Henrik Jensen, Applied Surface, 2005
Ti 2p	455.900	TiO	P.Madhu Kumar, Thin Films,2000
Ti 2p	456.700	Ti_2O_3	P.Madhu Kumar, Thin Films,2000
Ti 2p	485.500	TiO_2	P.Madhu Kumar, Thin Films,2000
Ti 2p	464.200	TiO_2	Nicola J.Price, 1999
Ti 2p	458.500	TiO_2	Nicola J.Price, 1999
Ti 2p	461.700	Ti_2O_3	Nicola J.Price, 1999
Ti 2p	456.100	Ti_2O3	Nicola J.Price, 1999
Ti 2p	464.280	TiO_2	Henrik Jensen, Applied Surface, 2005
Ti 2p	458.500	TiO_2	Henrik Jensen, Applied Surface, 2005
C 1s	288.400	C=C	Henrik Jensen, Applied Surface, 2005
C 1s	285.000	C-O (ref.)	Henrik Jensen, Applied Surface, 2005
C 1s	284.300	C-C	Henrik Jensen, Applied Surface, 2005

VITA

Mr.Supawut Phuphattarakul was born on June 20, 1982 in Kamphaengphet Province, Thailand. He received the Bachelor Degree of Chemical Engineering from Faculty of Engineering, Chulalongkorn University in 2004. In June 2004, he started his graduate study at department of Chemical Engineering, Chulalongkorn University.